Egypt. J. Chem. **Vol. 64,** No. 11 pp. 6647 - 6671 (2021)

Egyptian Journal of Chemistry

http://ejchem.journals.ekb.eg/

Metabolomic Profiling of *Sansevieria trifasciata* hort ex. Prain Leaves and Roots by HPLC-PAD-ESI/MS and its Hepatoprotective Effect via Activation of the NRF2/ARE Signaling Pathway in an Experimentally Induced Liver Fibrosis Rat Model

M. A. Raslan[a*], R. F. Abdel-Rahman[b], H. M. Fayed[b], H. A. Ogaly[c,d] and R. F. Taher[e]

[a] *Pharmacognosy Department, National Research Centre, Dokki, 12622 Giza, Egypt.*

[b] *Pharmacology Department, National Research Centre, Giza 12622, Egypt.*

[c] *Department of Biochemistry and Molecular Biology, Faculty of Veterinary Medicine, Cairo University, Giza 12211, Egypt*

[d] *Department of Chemistry, College of Science, King Khalid University, Abha 61421, Saudi Arabia*

[e] *Natural Compounds Chemistry Department, National Research Centre, Dokki, Giza, Egypt.*

Abstract

Sansevieria species show various bioactivities. Nevertheless, its therapeutic prospect in liver fibrosis even now is uninvestigated. The present study was conducted to analyze the metabolomic profile of *Sansevieria trifasciata* hort ex. Prain leaves and roots via HPLC-PAD-ESI/MS and evaluation of its hepatoprotective effect. The identified phytoconstituents were mainly steroidal saponins, phenolics and terpenoids. Sixty-one compounds were tentatively identified in StLE and fifty-nine compounds in StRE. Thioacetamide-induced liver fibrosis rat model was used to evaluate the hepatoprotective effect of *Sansevieria trifasciata* extracts via activation of the NRF2/ARE signaling pathway. Measurements of serum alanine transaminase (ALT), aspartate transaminase (AST) and malondialdehyde (MDA) were significantly decreased in treated groups with StLE and StRE (at doses of 200 and 100 mg/kg/day) compared with the TAA group. Also, the levels of reduced glutathione (GSH) content and hepatic mRNA levels of Nrf2, HO-1, NQO-1 and Keap-1 were markedly elevated. The prominent hepatoprotective effect was shown in StRE treated groups. Histological findings further confirmed the protective role of the plant against TAA-induced liver fibrosis. In conclusion, the abovementioned results indicated that the hepatoprotective mechanism of StLE and StRE could be achieved by activating Nrf2-ARE signaling pathways to alleviate oxidative stress and inflammation.

Keywords: *Sansevieria trifasciata*; Metabolite profiling; Liver fibrosis; thioacetaide; Nrf2, α-SMA.

1. Introduction

Liver fibrosis is a recoverable injury healing reaction of the liver, triggered by repeated and chronic liver injury. Various etiologies might be responsible for this such as dipsomania, fatty liver, long-term viral diseases, and ailments of biliary duct, autoimmune syndromes, and subjection to several toxicants [1, 2]. Quiescent hepatic stellate cells (HSCs) are activated and converted into myofibroblast-like cells in return for long-term liver damage. Activated HSCs exude abundant extracellular matrix (ECM) proteins and express the contractile protein α-smooth muscle actin (α-SMA) [3].

Previous studies have shown that oxidative stress is closely related to the progression of liver fibrosis, in which overproduction of free radicals may lead to destruction to structural and functional integrity of cells, resulting in major liver damage [4]. Furthermore, HSCs activation and collagen production can be promoted through free radicals and other reactive oxygen species (ROS) [5]. Consequently, establishing hepatoprotective therapies to lessen or stop ROS formation and to support physiological antioxidant potential will be a fruitful strategy in preventing liver fibrosis.

It was revealed that nuclear factor erythroid 2-related factor (Nrf2) as well as its negative regulator kelch-like ECH-associated protein 1 (Keap1) perform an important pathway in normal liver cells to combat oxidative stress [6]. Nrf2 is regarded as the main director of the antioxidant response element (ARE) that mediate detoxification and antioxidant gene

*Corresponding author e-mail: monaazzam78@gmail.com

Receive Date: 04 June 2021, Revise Date: 14 June 2021, Accept Date: 20 June 2021

DOI: 10.21608/EJCHEM.2021.78970.3877

expression [7]. Under normal circumstances, Nrf2 interrelates with Keap1 and is held in the cytoplasm. Responding to oxidative stress, Nrf2 separates from Keap1 and transfers to the nucleus, as it binds to ARE and subsequently induces expression of the downstream specific genes, including the quinone oxidoreductase 1 (NQO1), heme oxygenase (HO-1), and glutathione, as these perform a role against oxidative stress [8], 2008). Therefore, agents which can activate Nrf2 may be useful in alleviating oxidative stress-induced liver injury.

Medicinal plants have always been significant sources of hepatoprotective drugs. Silymarin, a hepatoprotective drug widely used, is a combination of flavonolignans isolated from the milk thistle *(Silybum marianum Gaertneri)* [9]. *Sansevieria* (Family: Asparagaceae) is a genus comprising about 60 xerophytic perennial species spread mainly in tropical and subtropical areas of Africa and Asia [10]. *Sansevieria* species are of great economic importance as ornamentals and as a good source of fibers. Moreover, it has been used as a folk remedy for curing different ailments [11]. *Sansevieria trifasciata* hort ex. Prain, commonly known as snake plant, is an evergreen perennial herb cultivated in Egypt for ornamental purposes. It has been used for traditional treatment of inflammatory conditions and snakebite in tropical America and South Africa [12]. Previous phytochemical studies reported the isolation of steroidal saponins [11,13–16], dihydrochalcones [16] and sappanin-type homoisoflavonoids [17] from *S. trifasciata* aerial parts. Several steroidal sapogenins, saponins, homoisoflavonoids, flavonoids and dihydrochalcones were formerly isolated from other *Sansevieria* species [18–23]. *Sansevieria trifasciata* was reported to possess analgesic, anti-inflammatory, antipyretic [24], antidiabetic [25], antiallergic [26] and thrombolytic activities [27]. Other *Sansevieria* species possessed antimicrobial [28], antioxidant [28,29], antitumor [20,22,23,28,30], antidiabetic [31], analgesic, anti-inflammatory, anti-ulcerative and hepatoprotective activities [32].

As far as we know, the effect of *Sansevieria trifasciata* in *in vivo* studies of on the Nrf2 signaling pathway in the TAA-induced liver fibrosis model was not inspected yet. As a part of our studies on plants cultivated in Egypt, we have investigated the phytoconstituents profile of *Sansevieria trifasciata* leaves and roots using HPLC–UV–ESI MS/MS and its effect on liver fibrosis by promoting the expression of Nrf2 and its downstream antioxidant enzymes in a rat model of TAA-induced hepatic fibrosis.

2. Experimental

2.1. Chemicals and Reagents

Acetonitrile and formic acid (HPLC grade) were obtained from Sigma-Aldrich (St. Louis, MO, USA). Water was purified using Milli-Q water purification system (Millipore, USA). Methanol (analytical grade) was obtained from Sigma-Aldrich (St. Louis, MO, USA). Thioacetamide (TAA) was obtained from El-Gomhouria Company for drugs and chemicals, Egypt. Alpha α-smooth muscle actin (α-SMA) were obtained from Cell Signaling Technology (Beverly, MA, USA).

2.2. Plant Material

The leaves and roots of *Sansevieria trifasciata* hort ex. Prain (family: Asparagaceae) were collected from Orman botanical garden, Giza, Egypt in June 2018, kindly authenticated by Dr Mohammed El-Gebaly, Department of Botany, National Research Centre. Voucher specimens (2018-25, 2018-26) were deposited in the Herbarium of National Research Centre.

2.3. Extraction

The air-dried powdered leaves (1 Kg) and roots (1Kg) of *Sansevieria trifasciata* hort ex. Prain was extracted separately. Each part of the plant was macerated twice with 70% aqueous methanol till exhaustion. The combined methanolic extract of each part was evaporated under vacuum to dryness.

2.4. HPLC-PDA- ESI-MS/MS Analysis

2.4.1. Sample Preparation

One mg of 70% methanolic extract of each part of the plant was dissolved in 1 mL 100% MeOH. After sonication for 2 min., each sample was centrifuged at 13000 rpm for 3 min. to remove insoluble material and the supernatant was then injected.

2.4.2. Apparatus and Conditions

Chromatographic analysis was performed at the UMASS-Amherst Mass Spectrometry Center (University of Massachusetts Amherst, Amherst, United States). Briefly, nanoLC-MS/MS was conducted in an Orbitrap Fusion Tribid mass spectrometer (ThermoFisher Scientific). The sample was separated in a nanoLC column (Thermo Acclaim PepMap RSLC column, 75 μm × 15 cm) with an Easy-nLC 1000 chromatography system (ThermoFisher Scientific, Massachusetts, United States)) using acetonitrile (A) and water (B) as mobile phase, with a gradient elution of 20–30% A at 0–10 min, 30–40% A at 10–30 min, 40–80% A at 30–50 min, and 80–95% A at 50–60 min. A 15 min re-equilibration time was used between HPLC runs. The solvent flow rate was 1.0mLmin−1 and the column temperature was ambient. The detection wavelength was set at 205-600 nm. The eluted phytoconstituents were analyzed with a resolution of 60 000 and a scan range of 200−1500 m/z. Tandem mass spectrometry was performed using collision-induced dissociation (CID) with a 35%

collision energy. The MS data were analyzed using Proteome Discoverer (ThermoFisher Scientific, Version 2.2).

2.4.3. Tandem Mass Spectrometry (MS-MS)

Precursor ions were selected and fragmented in the collision cell applying collision energies in the range of 10–30 eV. Argon was used as the collision gas. Product ions were detected using the following parameter settings: pulser frequency, 10 kHz; spectra rate, 1.5 Hz. For CID of in-source fragment ions, in-source CID energy was increased from 0 to 100 V. MS/MS spectra were obtained on Thermo Orbitrap Fusion instrument using the same elution gradient as in HPLC-MS. The system equipped with an ESI source (electrospray voltage 4.0 kV, sheath gas: nitrogen; capillary temperature: 275ºC) in negative ionization modes.

2.5. Hepatoprotective Effect:

2.5.1. Animals

Adult 42 male Wister rats weighed 150-180 g were utilized; they were obtained from the animal house colony at the National Research Centre, Giza, Egypt. Stainless steel-cages were used for housing the animals in a temperature of 25±0.5 °C, with suitable lighting conditions, humidity degree of 60% and good ventilation. Animals offered norm food pellets and tap water *ad libitum*. All animal procedures were done according to the protocol approved by the Institutional Ethical Committee of NRC (approval number: MREC-19-282).

2.5.2. Experimental Design

Forty-two rats were used to carry out the study and they were divided into seven groups (six animals each) as follows. Group 1 (control group): rats received the vehicle (saline). The remaining groups were subjected to liver fibrosis induction by intraperitoneal injection of thioacetamide (TAA) (200 mg/kg b.wt.) twice weekly for six successive weeks [33]. Group 2 served as (TAA group). Treated groups: Groups 3 and 4 were received *Sansevieria trifasciata* leaves' extract (StLE) at doses of 200 and 100 mg/kg/day, Groups 5 and 6 were treated with *Sansevieria trifasciata* roots' extract (StRE) at doses of 200 and 100 mg/kg/day respectively, two weeks before liver fibrosis induction and continued concomitantly with TAA injection. Group 7 (standard group): the rats received silymarin 100 mg/kg b.wt. daily two weeks before liver fibrosis induction and continued concomitantly with TAA injection.

At the end of the experimental period, blood samples were collected from the tail vein, clear sera were obtained. Livers of all animals were rapidly collected followed by washing in normal saline, blotted dry then weighed and divided into 2 portions; one was retained for the preparation of hepatic tissue homogenate; for further assessments of some antioxidant parameters, while the other part was kept in 10% neutral buffered formalin for further histopathological and immunohistochemical investigations.

2.5.3. Measurement of Some Serum Biochemical Parameters

Toassess liver injury caused by TAA administration, enzymatic activities of serum alanine transaminase (ALT) and aspartate transaminase (AST) were colourimetrically estimated by using the commercial diagnostic kits (Chema Diagnostica, Italy).

2.5.4. Measurement of Hepatic Levels of GSH, and MDA

Liver tissues were homogenized in ice-cold PBS buffer and then centrifuged at 10,000 ×g for 10 min at 4°C. Supernatants were collected for the measurement of hepatic reduced glutathione (GSH) and malondialdehyde (MDA) using the corresponding commercial assay kits (Cayman Chemical Company, Ann Arbor, MI, USA), according to the procedures stated in the manufacturer's manual.

2.5.5. Histopathological Examination

Liver tissue samples were dissected, fixed in 10% neutral buffered formalin for 72 hrs. Samples were processed in serial grades of ethanol, cleared in Xylene, tissue impregnation and embedding in Paraplast tissue embedding media. 4µn thick lung tissue sections were cut by rotatory microtome and mounted on glass slides and stained with H&E or Masson's trichrome stain for demonstration of collagen fibres. All methods of tissue samples preparation and staining as outlined by [34,35]. Six representative non-overlapping fields were randomly selected per tissue section of each sample for the determination of area percentage of collagen fibers deposition in Masson's trichrome stained sections.

Data were obtained using Full HD microscopic imaging system (Leica Microsystems GmbH, Germany) operated by Leica Application software for tissue sections analysis.

2.5.6. Immunohistochemical Examination

According to the manufacturer's protocol, deparaffinized 4µm thick tissue sections were treated by 3% H_2O_2 for 20 mins. Washed, then incubated with anti-alpha smooth muscle actin antibody (Abcam Ab5694 – 1:100) overnight; washed by PBS followed by incubation with secondary antibody HRP Envision kit (DAKO) 20 mins; washing by PBS and incubated with diaminobenzidine (DAB) for 10 mins. Washing by PBS then counterstaining with hematoxylin, dehydrated and clearing in xylene then cover slipped for microscopic examination. The percentage (%) of

the immunopositive stained area (dark brown) was calculated as the mean of 6 fields/slide.

2.5.7. RNA Extraction, cDNA Synthesis, and Reverse Transcription-Quantitative Polymerase Chain Reaction (RT-qPCR)

The mRNA transcript expression was determined for Nrf2, HO-1, Keap-1 and NQO genes using a standard real-time PCR. Total RNA was extracted from frozen liver samples using the QIAamp RNA mini kit (Qiagen, Germany) according to the instructions provided by the manufacturer. On column DNA digestion was done using QIAGEN's RNase-free DNase kit. RNA concentrations were quantified by a Nanodrop ND 1000 UV Spectrophotometer. A total of 1µg RNA was reverse transcribed into cDNA using RevertAidTM First Strand cDNA Synthesis Kit and a random primer (Fermentas). Real-time quantitative PCR was performed with SYBR Green Master Mix and specific oligonucleotide primer sets for Nrf2, HO-1, Keap-1, NQO, and the housekeeping gene β-actin (Table 3). PCR thermal program was performed as follows: an initial denaturation step at 95 °C for 10 min, followed by 40 cycles at 95 °C for 10 s, 56°C for 15 s and 72 °C for 20 s. For data analysis, the comparative delta-delta CT method ($2^{-\Delta\Delta CT}$) was used for relative quantification of the target gene as follows: ΔΔCT = (CT of the target gene − CT of β-actin) for treated sample − (CT of the target gene − CT of β-actin) for the calibrator (normal control). After validation of the method, results for each sample were expressed in fold changes in the target gene copies normalized to β-actin relative to the copy number of the target gene in calibrator according to the following equation: the amount of target = $2^{-\Delta\Delta CT}$. Statistical analysis was performed using SPSS (version 21) and $p \leq 0.05$ was considered statistically significant.

2.5.8. Statistical Analysis

The obtained data were expressed as the mean ± standard error (SE). Data were statistically analyzed using one-way analysis of variance (ANOVA), followed by Tukey's multiple comparison test using the GraphPad Prism program. Results were considered to be significant when *p* values ≤0.05.

3. Results and Discussion

3.1. Metabolites Profiling via HPLC- PAD-MS/MS Analysis

High-performance liquid chromatography (HPLC) represents a valuable tool for the rapid analysis of natural products. When coupled with UV and ESI-MS/MS tandem mass detectors, HPLC can invest phytoconstituents profiling of the plants. The MS/MS spectrum is a characteristic fingerprint for each phytoconstituent even if these metabolites have the same molecular formula [36]. In this study, a qualitative analysis of the phytoconstituents of 70 % aqueous methanolic extracts of *Sansevieria trifasciata* leaves and roots was performed using HPLC–PAD-ESI-MS/MS in negative ionization modes. As far as we know, this is the first study of complete fingerprint profiles of the leaves and roots of *Sansevieria trifasciata* and the consequent comparison between them. Figures 1 and 2 represent the HPLC-ESI-MS/MS base peak chromatograms of leaves' (StLE) and roots' extracts (StRE), respectively. Phytoconstituents has been preliminary identified through the comparison of their retention time Rt, UV information spectral and tandem mass (MS/MS) fragmentation model with literature data and online mass databases: Mass Bank database [37] and Mass Bank of North America (MoNA) [38]. Table 1 reveals the compounds preliminary identified using HPLC–PAD-ESI-MS/MS experiments together with their retention times (R_t), recognized molecular ions, UV λ_{max}, molecular formulas, MS/MS fragment ions, references used in the identification process and their presence in each extract. Sixty-one compounds were tentatively identified in StLE and fifty-nine compounds in StRE. The common compounds in both extracts were fifty-four compounds. Seven compounds were only characterized in StLE. Five compounds were only found in StRE.

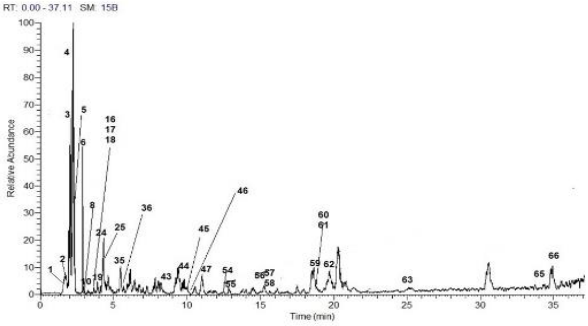

Figure 1: HPLC-ESI-MS/MS chromatogram of *S. trifasciata* hort ex. Prain leaves 70% aqueous methanolic extract (StLE).

3.1.1. Steroidal Saponins

Steroidal saponins are considered from the most characteristic metabolites of genus *Sansevieria* [39]. Steroidal saponins previously isolated from *Sansevieria* species were mainly pregnane steroidal saponin, spirostane steroidal saponin, furostane steroidal saponins, and cholestane steroidal saponin [11,14–16,20,22,23]. Twenty and sixteen steroidal saponins were detected in StLE and StRE, respectively, 15 of them were common in both extracts. The identification of them was supported by the MS data of steroidal saponins previously reported in the literature (Table 2).

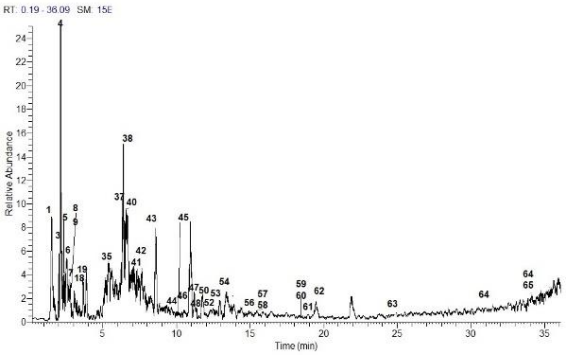

Figure 2: HPLC-ESI-MS/MS chromatogram of *S. trifasciata* hort ex. Prain roots 70% aqueous methanolic extract (StRE). The common steroidal saponins identified in both extracts were mainly 11 saponins previously isolated from *S. trifasciata* and 1 saponin previously isolated from other members of family Asparagaceae. Since the shortage of experimentally collected steroidal saponins reference spectra, the identification of them was confirmed using Competitive Fragmentation Modeling-ID (CFM-ID)[40–42]. Five more peaks were detected in StLE only; four of them were previously isolated from *S. trifasciata*. The detected steroidal saponins were classified into three types, pregnane, spirostane and furostane steroidal saponins. In negative ion mode ESI, saponins produce deprotonated molecular ions $[M-H]^-$ and MS/MS daughter fragments attributed to the loss of saccharide units. Some saponins produce a formate adduct ion $[M+HCOO]^-$ [43].

3.1.1.1. Pregnane Steroidal Saponin

Peaks 8, 33 and 5 were detected in both extracts. They produced the molecular ions $[M-H]^-$ at m/z 769, 739 and 811, respectively. The MS/MS spectrum of the forementioned peaks showed a characteristic ion at m/z 329 representing dihydroxypregna-5,16-dien-20-one 1-one aglycone. The molecular ion $[M-H]^-$ at m/z 769 gave daughter fragments attributed to the loss of deoxyhexose, pentose and hexose units at m/z 769 $[M-H]^-$, 751 $[M-H-H_2O]^-$, 637 $[M-H-132]^-$, 623 $[M-H-146]^-$ and 329 $[Aglycone-H]^-$, thus was characterized as dihydroxypregna-5,16-dien-20-one deoxyhexoside pentoside hexoside (Supplementary figure 8). While the molecular ion $[M-H]^-$ at m/z 739 gave daughter fragments attributed to the loss of deoxyhexose and two pentose units at m/z 739 $[M-H]^-$, 721 $[M-H-H_2O]^-$, 593 $[M-H-146]^-$,607 $[M-H-132]^-$, 461 $[M-H-146-132]^-$ and 329 $[Aglycone-H]^-$, suggesting its characterization as dihydroxypregna-5,16-dien-20-one deoxyhexoside dipentoside (Supplementary figure 33). The molecular ion $[M-H]^-$ at m/z 811 gave daughter fragments similar to those of the molecular ion $[M-H]^-$ at m/z 769 with the difference of 42 Da suggesting the presence of acetyl group on the hexose unit. Hence, it was tentatively identified as dihydroxypregna-5,16-dien-20-one deoxyhexoside pentoside acetyl hexoside (Supplementary figure 5). The isolation of 1β,3β-dihydroxypregna-5,16-dien-20-one 1-O-{O-α-L-rhamnopranosyl-(1→2)-O-[β-D-xylopyranosyl-(1→3)]-β-D-glucopyranoside}, 1 β,3 β -Dihydroxypregna-5,16-dien-20-one 1-O- {α -L-rhamnopyranosyl-(1→2)- [β -D-xylopyranosyl-(1→3)]-α -L-arabinopyranoside} and 1β,3β- dihydroxypregna-5,16-dien-20-one 1-O-{O-α-L-rhamnopranosyl-(1→2)-O-[β-D-xylopyranosyl-(1→3)]-6-O-acetyl-β-D-glucopyranoside} from *S. trifasciata* was previously reported supporting the suggested identification of peaks 8, 33 and 52, respectively [15] (Table 2).

3.1.1.2. Spirostane Steroidal Saponin

Fourteen and eleven spirostane steroidal saponins were detected in StLE and StRE, respectively, with ten common ones. The following ten peaks were detected in both extracts and produced MS data similar to spirotane derivatives previously isolated from *S. trifasciata*. Peaks 1 and 42 produced the molecular ions $[M-H]^-$ at m/z 1157 and 953, respectively. The MS/MS spectrum of these peaks showed a characteristic ion at m/z 459. Peak 1 produced fragment ions at m/z 1157 $[M-H]^-$, 1139 $[M-H-H_2O]^-$, 1115 $[M-H-Ac]^-$, 885 [M-146-3Ac], 459 $[Aglycone-H]^-$, corresponding to the loss of four saccharide units, triacetyl deoxy hexose, two pentose and hexose units, respectively. While peak 42 MS/MS ions indicated the loss of three saccharide units, diacetyl deoxyhexose and two pentose units. Peaks 1 and 42 were tentatively identified as tetrahydroxy spirosta-diene-triacetyldeoxyhexoside dipentoside hexoside and tetrahydroxy spirosta-diene-diacetyldeoxyhexoside dipentoside, respectively (Supplementary figures 1 and 42). (23S,24S)-spirosta-5,25(27)-diene-1β,3 β ,23,24-tetrol-1-O-{O-(2,3,4-O-triacetyl-α-L-rhmnopyranosyl)-(1→2)-O-[β-D-xylopyranosyl-(1→3)]-α-L-arabinopyranoside}24-O- β-D-glucopyranoside and (23S,24S)-spirosta-5,25(27)-diene-1β,3 β ,23,24-tetrol-1-O-{O-(2,3-O-diacetyl-α-L-rhamnopyranosyl) -(1→2)-O-[β-D-xylopyranosyl-(1→3)]-α-L-arabinopyranoside} were previously isolated from *S. trifasciata* [14] (Table 2). Peaks 34 and 44 with the molecular ions $[M-H]^-$ at m/z 937 and 853, respectively, produced the characteristic fragment ion at m/z 443. Both showed fragmentation pattern suggesting the loss of deoxyhexose unit (-146 Da) and two pentose units (-2 X 132 Da). A mass difference of 84 Da, suggests the presence of two acetyl moieties in Peak 34. Peaks 34 and 44 were tentatively identified as trihydroxy spirosta-diene- diacetyl deoxyhexoide dipentoside and trihydroxy spirosta-diene- deoxyhexoide dipentoside, respectively (Supplementary figures 34 and 44). This identification is supported by the reported isolation of (23S)-spirosta-5,25(27)-diene-1 β,3 β,23-triol-1-O-{O-(2,3-O-diacetyl-α-L-rhamnopyranosyl) -(1→2)-O[β-D-xylopyranosyl-(1→3)]-α-L-arabinopyranoside} and (23S)-spirosta-5,25(27)-diene-β,3 β,23-triol-1-O-{O-α-L-rhamnopyranosyl-(1→2)-O-[β-D-xylopyranosyl-(1→3)]-α-L-arabinopyranoside} from *S. trifasciata* [14]. Peak 50 with the molecular ion $[M-H]^-$ at m/z 869 showed the fragment ion at m/z 429 $[Aglycone-H]^-$, the loss of deoxyhexose unit (-146 Da),

the loss of hexoside unit (-162 Da) and the loss of pentoside unit (-132 Da) (Supplementary figure 50). Thus, peaks 50 was tentatively characterized as hydroxyspirost-en deoxyhexoside pentoside hexoside. Its MS data resembles the data of trifasciatoside C previously isolated from *S. trifasciata*. The molecular ions $[M-H]^-$ at m/z 429 (Peak 65) and 427 (Peak 66) were identified as the characteristic constituents of *S. trifasciata*, neoruscogenin and ruscogenin, respectively [13,44] (Supplementary figure 65).

The following 3 peaks were detected in both extracts and produced MS data similar to spirotane derivatives previously isolated from family Asparagaceae. Peak 5 along with the molecular ion $[M-H]^-$ at m/z 837 showed the characteristic neoruscogenin aglycon at m/z 427 (Supplementary figure 5). Neoruscogenin derivatives were previously isolated from family Asparagaceae (Table 2) [45–47]. According to this literature data, and MS/MS fragmentation (Table 1), peak 5 was tentatively characterized as neoruscogenin deoxyhexoside dipentoside. Moreover, peaks 5 and 45 along with molecular ions $[M-H]^-$ at m/z 925 and 741, respectively, have been tentatively characterized as Tetrahydroxyspirosta-dien acetyldeoxyhexoside pentoside deoxyhexoside and Trihydroxyspirostane hexoside pentoside, respectively, according to their MS/MS data (Table 1) and the literature data of spirostan derivatives previously isolated from Asparagaceae family [48,49].

On the other hand, 4 peaks; 2, 39, 51 and 59, with molecular ions $[M-H]^-$ at m/z 1141, 1099, 895 and 911, respectively, have been detected only in StLE (Supplementary figures 2, 39, 51 and 59). The molecular ion $[M-H]^-$ at m/z 1141 (Peak 2) produced MS/MS spectrum with the characteristic ion at m/z 459 similar to Peaks (39 and 59) with the loss of triacetyldeoxyhexose, two pentose and deoxyhexose units. It was assigned as tetrahydroxy spirosta-diene triacetyldeoxyhexoside dipentoside deoxyhexoside . Peak 39 with the molecular ion $[M-H]^-$ at m/z 1099 showed similar MS/MS data with less 42 Da suggesting its identification as tetrahydroxy spirosta-diene- diacetyl deoxyhexoside dipentoside deoxyhexose. While peak 59 showed the loss of one acetyl, deoxyhexose and 2 pentose units. It was identified as tetrahydroxy spirosta-diene acetyl deoxyhexoside dipentoside. (23S,24S)-spirosta-5,25(27)-diene-1β,3 β ,23,24-tetrol-1-O-{O-(2,3,4-O-triacetyl-α-L-rhmnopyranosyl)-(1→2)-O-[β-D-xylopyranosyl-(1→3)]-α-L-arabinopyranoside}24-O-rhamnopyranoside, (23S,24S)-spirosta-5,25(27)-diene-1β,3 β ,23,24-tetrol-1-O-{O-(2,3,4-O-triacetyl-α-L-rhmnopyranosyl)-(1→2)-O-[β-D-xylopyranosyl-(1→3)]-α-L-arabinopyranoside}24-O-fucopyranoside, (23S,24S)-spirosta-5,25(27)-diene-1β,3 β ,23,24-tetrol-1-O-{O-(2,3-O-diacetyl-α-L-rhmnopyranosyl)-(1→2)-O-[β-D-xylopyranosyl-(1→3)]-α-L-arabinopyranoside}24-O- β-D-fucopyranoside and (23S,24S)-spirosta-5,25(27)-diene-1β,3 β ,23,24-tetrol-1-O-{O-(4-O-acetyl-α-L-rhmnopyranosyl)- (1→2)-O- [β-D-xylopyranosyl-(1→3)]-α-L-arabinopyranoside} were previously isolated from *S. trifasciata* [14]. The molecular ion $[M-H]^-$ at m/z 895 (Peak 51) produced MS/MS spectrum with the characteristic loss of acetyl, deoxyhexose and two pentose units. Thus, it was identified as trihydroxy spirosta-diene acetyl deoxyhexoside dipentoside. (23S)-spirosta-5,25(27)-diene-1 β,3 β,23-triol-1-O-{O-(4-O-acetyl-α-L-rhamnopyranosyl) -(1→2)-O- [β-D-xylopyranosyl-(1→3)]-α-L-arabinopyranoside} were previously isolated from *S. trifasciata* [14].

Peak 7 was detected only in StRE and produced MS data similar to spirotane derivatives previously isolated from the family Amaryllidaceae, closely related to family Asparagaceae. Peak 7 produced the molecular ion $[M-H]^-$ at m/z 965, daughter fragments at m/z 803 $[M-H-162]^-$, 641 $[M-H-162-162]^-$, 479 $[M-H-162-162-162]^-$ (Supplementary figure 7) suggesting its identification as pentahydroxy spirostane trihexoside. This data is similar to the reported MS data of (24S,25S)-5α-Spirostane-2α,3β,5,6β,24-pentol 2-O-{β-D-glucopyranoside-24-O-β-D-glucopyranosyl-(1→2)-β-D-glucopyranoside} previously isolated from *Allium karataviense* (F. Amaryllidaceae) [50].

3.1.1.3. Furostane Steroidal Saponins

Two furostane derivatives were detected in both extracts. The molecular ion $[M-H]^-$ at m/z 1063 detected at R_t 4.63 min. produced the fragment ions at m/z 931 $[M-H-132]^-$, 755 $[M-H-162-146]^-$, 623 $[M-H-162-146-132]^-$, 461 $[Aglycone-H]^-$ (Supplementary figure 29). According to literature, trifasciatoside F with the structure, 26-[(β-D-glucopyranosyl) oxy]-3β-hydroxy-22α-methoxy-(25S)-furost-5-en-1β-yl-O-α-L-rhamnopyranosyl-(1→2)-O-[β-D-xylopyranosyl-(1→3)]-β-D-glucopyranoside, previously isolated from *S. trifasciata*, had similar MS data [11]. Therefore, peak 29 was suggested to be trihydroxyfurost-en deoxyhexoside pentoside dihexoside. Reviewing the literature, peak 54 along with the molecular ion $[M-H]^-$ at m/z 835 was tentatively identified as hexahydroxy methoxyfurostane dihexoside due to similarity of MS data with furostane derivatives commonly found in Asparagaceae family (Compounds 54) (Table 2) [51]. On the other hand, peak 49 along with the molecular ion $[M-H]^-$ at m/z 1075 was detected only in StLE. It produced the fragments at m/z 929 $[M-H-146]^-$, 751 $[M-H-2X\ 162]^-$, 605 $[M-H-146-2X162]^-$ (Supplementary figure 49), similar to the MS data of

dioscoreside E, (23S,25R)-23-Methoxyfurost-5,20(22)-diene 3,26-diol 3-O- {α -L-rhamnopyranosyl-(1→2)- [β -D-glucopyranosyl-(1→3)- β -D-glucopyranoside}-26-O- β -D-glucopyranoside, suggesting its identification as dihydroxy methoxyfurost--diene deoxyhexoside trihexoside [52].

3.1.2. Phenolics

3.1.2.1. Phenolic Acids and Phenolic Acid Derivatives

Six phenolic acid derivatives were tentatively identified in StLE and StRE. Moreover, three phenolic acid derivatives were only detercted in StRE.

3.1.2.1.1. Benzoic Acid Derivatives

The molecular ion $[M-H]^-$ m/z 315 detected in both extracts at 15.01 min. (peak 56) gave MS/MS spectrum resembling the characteristic fragments at m/z 153 $[M-H-162]^-$ and 109 $[M-H-162-44]^-$, that are compatible with the misplacement of hexose and CO_2 moieties, respectively (Supplementary figure 56). Therefore, peak 56 has been proposed as protocatechuic acid hexoside [53]. On the other hand, peak 37 with molecular ion m/z 377 was found only in the roots' extract. Peak 37 produced an MS/MS spectrum characteristic to benzoic acid derivative as compared to MassBank of North America (MoNA) and thus it was tentatively characterized as methyl 4-[1,3-dihydroxy-1-(4-hydroxy-3-methoxyphenyl) propan-2-yl] oxy-3-methoxybenzoate [38] (Supplementary figure 37).

3.1.2.1.2. Cinnamic Acid Derivatives

Five cinnamic acid derivatives were detected in both extracts. The molecular ion $[M-H]^-$ m/z 487 detected at 3.32 min. showed MS/MS spectrum with the characteristic ions at m/z 308 $[M-H-179]^-$, 294 $[M-H-193]^-$, and 193 due to the misplacement of caffeic acid moiety, loss of ferulic acid moiety and ferulic acid ion, respectively. It was tentatively identified as caffeoyl–feruloyltartaric acid [37] (Supplementary figure 12). The molecular ion $[M-H]^-$ m/z 337 detected at 4.07 min. showed MS/MS spectrum with the characteristic ions at m/z 191, 173, 163, 119. It was characterized as coumaroylquinic acid [54] (Supplementary figure 21). The molecular ion $[M-H]^-$ m/z 353 detected at 15.85 min. showed the characteristic ions at m/z 309 $[M-H-44]^-$, 191 and 161 $[M-H-191]^-$ corresponding to the loss of CO_2, deprotonated quinic acid ion, and loss of quinic acid moiety, respectively. It was characterized as Chlorogenic acid [55] (Supplementary figure 57). The molecular ion $[M-H]^-$ m/z 371 detected at 11.16 min. was preliminary identified as hydroxy-dihidrocaffeolyquinic acid, as it shows peaks equivalent to caffeolyquinic acids (m/z 353, 191, 179, 135), still have a characteristic ion at m/z 371 (Supplementary figure 47). The difference in masses between 371 and 353 = 18 m/z was determined by the presence of extra two H atoms and one O atom added to chlorogenic acid structure [56]. The molecular ion $[M-H]^-$ m/z 529 detected at 19.91 min. showed MS/MS spectrum with the characteristic ions at m/z 486 $[M-H-44]^-$,338 $[M-H-191]^-$, 179 and 159 $[M-H-191-179]^-$ corresponding to the loss of CO_2, quinic acid moiety, deprotonated caffeic acid ion and loss of quinic and caffeic acids moieties, respectively. It was characterized as caffeoyl–feruloylquinic acid [57] (Supplementary figure 7) (Supplementary figure 62). While the molecular ions $[M-H]^-$ at m/z 367 and 311 were detected only in StRE at 2.99 and 31.08 min., respectively. The molecular ion $[M-H]^-$ at m/z 367 gave the main fragment mass MS_2 at m/z 193 (for ferulic acid) and characterized as feruloylquinic acid [37] (Supplementary figure 9). While the molecular ion $[M-H]^-$ at m/z 311 gave the daughter fragments at m/z 293, 274, 183, 157, 130 and 119. It was characterized as caftaric acid [58] (Supplementary figure 64).

3.1.2.2. Flavonoids Derivatives

A sum of 23 and 23 flavonoid derivatives have been spotted and tentatively identified in StLE and StRE extracts, respectively, while 22 compounds were common in both extracts.

3.1.2.2.1. Chalcones

The molecular ion $[M-H]^-$ at m/z 255 detected at 13.89 min. in StLE with its major fragments at m/z 238, 226, 211 and 186 was characterized as trihydroxychalcone [37] (Supplementary figure 38).

3.1.2.2.2. Flavones and Flavanols

Eight compounds were common in both extracts. The molecular ions $[M-H]^-$ m/z 593, 577 and 431 (Peaks 4, 11 and 17, respectively) were detected in both extracts. Their MS/MS spectra have shown the typical product ions of isovitexin at m/z 431, 413, 341 and 311. UV chromatogram with λ_{max} at 268 and 335 nm was detected for peak 70. According to the previous literature [55,59], these compounds have been characterized as isovitexin hexoside, isovitexin deoxyhexoside and isovitexin, respectively.

Peak 48 (R_t 11.39 min.) with the molecular ion $[M-H]^-$ m/z 299 and the UV chromatogram with λ_{max} at 254, 295 and 337 nm was detected in both extracts. In the MS/MS spectrum, this compound produced daughter fragments at m/z 281 $[M-H-H_2O]^-$, 269 $[M-CH_3O]^-$ and 253 $[M-H-C_2H_6O]^-$ (Supplementary figure 48). It has been tentatively proposed as isokaemferide (5,7,4`-trihydroxy-3-methoxyflavone) [21]. Isokaemferide was previously isolated from *S. hyacinthoides* rhizomes [21]. Two hydroxy methoxy flavones were detected in both extracts at R_t 3.42 and 18.96 min. They were tentatively characterized as

scaposin and acacetin, respectively [37]. The molecular ion $[M-H]^-$ m/z 461 gave the daughter fragments at m/z 443, 371, 349, 332 and 299 along with the characteristic UV absorption of flavones (Supplementary figure 18). It has been tentatively assigned as scoparin [37]. Peak 30 was detected in both extracts. It showed λ_{max} 285 nm, $[M-H]^-$ ion at m/z 451, along with MS/MS ions at m/z 289 and 177 (Supplementary figure 30). It was tentatively identified as catechin hexoside [60]. Peak 23 with the molecular ion $[M-H]^-$ m/z 797 at R_t 4.22 min. was detected only at StLE. It showed the characteristic UV absorption and the characteristic product ions of apigenin (Supplementary figure 23). It was tentatively identified as 4'-O-(2'-feruloylglucuronyl) -(1-2)-glucuronyl apigenin [37]. While 7,4'-dimethoxy-3-hydroxyflavone ($[M-H]^-$ m/z 297 and λ_{max} at 289 nm was only detected in StRE at R_t 12.61 min. [37].

3.1.2.2.3. Flavanones and Isoflavones

Peaks 38, 43 and 60 possessing characteristic UV spectra, $[M-H]^-$ fragments at m/z 255, 611 and 315, and characteristic daughter ions (Table 1) were tentatively characterized as the flavanone derivatives, pinocembrine, eriodictyol dihexoside, and 5,7-dihydroxy-3',4'-dimethoxyflavanone, respectively [37,38,61]. The molecular ion $[M-H]^-$ m/z 407 detected in both extracts at R_t 4.40 min. (Peak 26) (Supplementary figure 26). Comparing its mass data and UV data, it was tentatively characterized as 6a,12a-didehydroamorphigenin [37].

3.1.2.2.4. Flavonols

Eight flavonoles were detected in both extracts. They were mainly kaempferol and quercetin derivatives. Kaempferol aglycone (Peak 63) and 2 kaempferol glycosides (Peaks 27 and 40) were detected in both extracts. Their MS/MS spectra showed the typical fragmentation pattern at m/z 285, 255 and 178 and their UV chromatograms showed characteristic absorption of kaempferol (Supplementary figure 27 and 40). Peaks 27 and 40 showed $[M-H]^-$ at m/z 447 and 593, respectively. They have been preliminary identified as kaempferol hexoside (Peak 27) and kaempferol hexoside deoxyhexoside (Peak 40), according to the loss of hexosyl (-162 Da) and the loss of hexosyl (-162 Da) and deoxyhexosyl (-146 Da) moieties, respectively [37,38]. Peak 25 with $[M-H]^-$ at m/z 505 showed characteristic fragments and UV absorption of quercetin and was identified as quercetin acetyl-hexoside [62]. The molecular ion $[M-H]^-$ at m/z 609 have been recognized as rutin according to its fragment ions and UV absorption [63]. Peaks 31 and 35 detected in both extracts, showed $[M-H]^-$ ions at m/z 639 and 623, respectively, λ_{max} 250 and 342 nm and misplacement of various glycoside moieties leading to formation of isorhamnetin aglycone (m/z 315). Thus, were tentatively assigned as isorhamnetin dihexoside and isorhamnetin rutinoside, respectively [37,64,65]. The molecular ion $[M-H]^-$ at m/z 301 (Peak 58) with the characteristic fragment ions at m/z 283, 273, 239, 195, 167, 125 was identified as hesperetin [37] (Supplementary figure 58).

3.1.2.2.5. Homoisoflavanones

Homoisoflavonoids are a group of naturally occurring oxygen heterocyclic compounds with a 16-carbon skeleton, that incorporate a chromanone, chromone or chromane system with a benzyl moiety at position C-3. Their presence in nature is restricted to certain plant families, Hyacinthaceae, Liliaceae, Asparagaceae, Fabaceae, Agavaceae, and Polygonaceae [66]. Two peaks were detected in both extracts and characterized as homoisoflavanones. Peak 24 (at R_t 4.30 min.) possessed the molecular ion $[M-H]^-$ at m/z 327 and λ_{max} 287 nm. Trifasciatine A, ((3R)-7-hydroxy-8-methoxy-3`,4`-methylene-dioxyhomoisoflavanone, previously isolated from *S. trifasciata* aerial parts) has the same molecular weight and UV absorption [17]. Moreover, peak 24 produced the MS/MS ions at m/z 283, 227, 191 and 161, which match the fragmentation pattern of type II homoisoflavonoids as previously described by [67]. Therefore, peaks 24 was tentatively assigned as trifasciatine A. Peak 36 showed $[M-H]^-$ ion at m/z 341 and similar UV data and MS/MS fragments to peak 24, thus It was identified as methylophiopogonanone A [68]. Notably, this homisoflavonoid was previously reported in Asparagaceae family [68].

3.1.2.3. Stilbenes

Stilbenes, a group of bioactive complex polyphenols, naturally found in limited but heterogeneous distribution through the plant kingdom. Asparagales order, where family Asprgaceae belongs, was reported as a source of stilbenes [69]. A stilbenoid derivative was detected in both extracts. Peak 20 produced the molecular ion $[M-H]^-$ at m/z 391, daughter fragments at m/z 373, 347, 304, 247, 223 and λ_{max} at 277 nm. According to the MassBank of North America (MoNA), peak 20 was tentatively characterized as 3-[(2E)-3,7-dimethylocta-2,6-dienyl]-2,4-dihydroxy-6-[(E)-2-phenylethenyl] benzoic acid [38].

Table 1: Compounds tentatively identified by HPLC-DAD-MS/MS of *Sansevieria trifasciata* hort ex. Prain leaves extract (StLE) and roots extract (StRE).

Peak No.	R_t. (min.)	StLE	StRE	[M-H]-	Formula	UV	Tentative Identification	Main fragments	Class	References
1	1.58	+	+	1157.3225	$C_{55}H_{82}O_{26}$	-	Tetrahydroxy spirosta-diene-triacetyldeoxyhexoside dipentoside hexoside	1157[M-H]$^-$,1139.2667[M-H-H_2O]$^-$,1115.9213[M-Ac]$^-$, 977.3667 [M-H-H_2O-162]$^-$, 885.3601[M-146-3Ac]$^-$, 723.7334 [M-H-146-3 Ac -162]$^-$, 459.8431 [Aglycone-H]$^-$	Spirostane steroidal saponin	[14]
2	1.98	+	-	1141.2997	$C_{55}H_{82}O_{25}$	-	Tetrahydroxy spirosta-diene-triacetyl deoxyhexoside dipentoside deoxyhexose	1141[M-H]$^-$,1055.0334 [M-2 Ac]$^-$, 866.3501 [M-146-3 Ac]$^-$, 737.8021 [M-146- 3 Ac - 132]$^-$, 605.3000 [M-146- 3 Ac- 132-132]$^-$	Spirostane steroidal saponin	[14]
3	2.08	+	+	503.118	$C_{18}H_{32}O_{16}$	-	Raffinose	340.9667,322.9667, 221.000, 179.0000	Sugar	[37]
4	2.11	+	+	593.7000	$C_{27}H_{30}O_{15}$	-	Isovitexin hexoside	615.1505 [M+Na-2H]$^-$, 503.1000, 435.0667, 413.06667, 341.0000	Flavone	[59]
5	2.46	+	+	925.2264	$C_{46}H_{70}O_{19}$	--	Tetrahydroxyspirosta-dien acetyldeoxyhexoside pentoside deoxyhexoside	925.2264 [M-H]$^-$, 883.1667 [M-H-Ac]$^-$, 736.2667 [M-H-Ac-146]$^-$, 604.8667 [M-H-Ac-146-132]$^-$	Spirostane steroidal saponin	[48]
6	2.86	+	+	345.0928	$C_{15}H_{22}O_9$	---	Aucubin	327.0333, 300.9333, 166.7333, 139.2000	Terpenoid	[38]
7	2.90	-	+	965.3987	$C_{45}H_{74}O_{22}$	-	Pentahydroxy spirostane trihexoside	965.3987 [M-H]$^-$, 803.4000 [M-H-162]$^-$, 641.4333 [M-H-162-162]$^-$, 479.7667 [M-H-162-162-162]$^-$	Spirostane steroidal saponin	[50]
8	2.99	+	+	769.2123	$C_{38}H_{58}O_{16}$	-	Dihydroxypregna-5,16-dien-20-one deoxyhexoside pentoside hexoside	769.2123 [M-H]$^-$, 751.2333 [M-H-H_2O]$^-$, 637.3333 [M-H-132]$^-$, 329.6667 [Aglycone-H]$^-$	Pregnane steroidal saponin	[15]
9	2.99	-	+	367.1576	$C_{17}H_{20}O_9$	----	feruloylquinic acid	349.1000, 323.1333, 292.9333, 191.3667, 161.0667	Cinnamic acid derivative	[54]
10	3.04	+	+	837.1857	$C_{43}H_{66}O_{16}$	-	Neoruscogenin deoxyhexoside dipentoside	837.1857 [M-H]$^-$, 690.4667 [M-H-146]$^-$, 559.2334 [M-H-132-146]$^-$, 427.8667 [Neoruscogenin-H]$^-$	Spirostane steroidal saponin	[45]
11	3.21	+	+	577.2451	$C_{27}H_{30}O_{14}$	-	Isovitexin deoxyhexoside	559.1334, 436.9333, 415.1000,	Flavone	[59]

								415.1000, 311.0667, 282.1000		
12	3.32	+	+	487.1413	$C_{23}H_{20}O_{12}$	-	caffeoyl–feruloyltartaric acid	322.9000, 307.0333, 300.8333	Cinnamic acid derivative	[57]
13	3.42	+	+	389.1689	$C_{19}H_{18}O_9$	281	Scaposin	371.7000, 361.9000, 353.1333, 343.1333	Flavone	[37]
14	3.44	+	+	511.1272	$C_{23}H_{28}O_{13}$	275	Picroside II	489.0333, 479.0000, 371.0000, 348.8667, 168.8667	Terpenoid	[38]
15	3.53	+	+	457.1299	$C_{27}H_{38}O_6$	-	Lucidenic acid A	439.2666, 419.1333, 411.1000, 399.0000, 332.3000, 293.0667, 163.1333	Terpenoid	[76]
16	3.60	+	+	585.2084	$C_{25}H_{30}O_{16}$	264, 347	Hydroxyhispidin dihexoside	423.2333, 379.0000, 263.9333	Glucopyranoside	[83]
17	3.61	+	+	431.1517	$C_{21}H_{20}O_{10}$	268, 335	Isovitexin	413.1000, 344.1000, 313.1333, 263.5000	Flavone	[55,59]
18	3.70	+	+	461.1261	$C_{22}H_{22}O_{11}$	272, 316	Scoparin (Chrysoeriol 8-C-glucoside)	443.0666, 371.1000, 349.0667, 332.0667, 299.3000	Flavone	[37]
19	3.83	+	+	247.1163	$C_{15}H_{20}O_3$	-	Pechueloic acid	203.0667, 172.9333, 110.9667	Terpenoid	[38]
20	4.01	+	+	391.1363	$C_{25}H_{28}O_4$	277	3-[(2E)-3,7-dimethylocta-2,6-dienyl]-2,4-dihydroxy-6-[(E)-2-phenylethenyl] benzoic acid	373.1667, 347.0333, 314.9000, 245.6333, 224.9000	Stilbene	[38]
21	4.07	+	+	337.0534	$C_{16}H_{18}O_8$	240, 320	Coumaroylquinic acid	190.7333, 172.7000, 163.0000	Cinnamic acid derivative	[54]
22	4.18	+	+	325.0898	$C_{15}H_{18}O_8$	-	Coumaric acid hexoside	307.1000, 163.0667	Coumarin glycosides	[55]
23	4.22	+	-	797.1596	$C_{37}H_{34}O_{20}$	285, 309	4'-O-(2'-Feruloylglucuronyl)-(1-2)-glucuronyl Apigenin	600.1666, 528.6000, 389.9667, 306.0000, 251.5000	Flavone	[37]
24	4.30	+	+	327.3054	$C_{18}H_{16}O_6$	287	Trifasciatine A ((3R)-7-hydroxy-8-methoxy-3`,4`-methylene-dioxyhomoisoflavanone)	283.0333, 227.8667, 191.6667, 160.8333	Homoisoflavanone	[17,67]
25	4.39	+	+	505.1337	$C_{23}H_{22}O_{13}$	-	Quercetin acetyl-hexoside	487.0667, 473.1000, 459.0334, 307.1333	Flavonol	[62]
26	4.40	+	+	407.0406	$C_{23}H_{20}O_7$	219, 268	6a,12a-Didehydroamorphigenin	389.9667, 375.0667, 363.1667, 210.9333, 122.8000	Isoflavone	[37]
27	4.54	+	+	447.0887	$C_{21}H_{20}O_{11}$	254,325, 357	Kaempferol hexoside	429.0666, 285.1000	Flavonol	[37]

28	4.60	+	+	609.1412	$C_{27}H_{30}O_{16}$	256,354	Rutin	464.1666, 296.1667	Flavonol	[63]
29	4.63	+	+	1063.484	$C_{51}H_{84}O_{23}$	-	Trihydroxyfurost-en deoxyhexoside pentoside dihexoside	1063.4840 $[M-H]^-$, 931.6000$[M-H-132]^-$, 755.4667 $[M-H-162-146]^-$, 623.000 $[M-H-162-146-132]^-$, 461.2333 $[Aglycone-H]^-$	Furostane steroidal saponins	[11]
30	4.75	+	+	451.133	$C_{21}H_{24}O_{11}$	280	Catechin hexoside	433.2667, 289.1000, 177.1000	Flavanol	[60]
31	4.77	+	+	639.1509	$C_{28}H_{32}O_{17}$	250, 342	Isorhamnetin dihexoside	520.3000, 475.4666, 315.9333, 304.4333	Flavonol	[64,65]
32	4.88	+	+	421.1595	$C_{24}H_{22}O_7$	268	6-((6-ethyl-4-hydroxy-5-methyl-2-oxo-2H-pyran-3-yl) methyl)-5,7-dihydroxy-2-phenylchroman-4-one	375.0333, 297.6333, 246.2667, 173.9667	Coumarin glycosides	[38]
33	5.02	+	+	739.1511	$C_{37}H_{56}O_{15}$	-	Dihydroxypregna-5,16-dien-20-one deoxyhexoside dipentoside	739.1511 $[M-H]^-$, 721. 0333 $[M-H-H_2O]^-$, 593.6333 $[M-H-146]^-$,607.1000 $[M-H-132]^-$, 461.0000 $[M-H-146-132]^-$, 329.8333 $[Aglycone-H]^-$	Pregnane steroidal saponin	[15]
34	5.12	+	+	937.2328	$C_{47}H_{70}O_{19}$	-	Trihydroxyspirosta-diene-diacetyl deoxyhexoside dipentoside	937.2328 $[M-H]^-$, 894.000 $[M-H-Ac]^-$, 853.9000 $[M-H-2Ac]^-$,707.0334 $[M-H-146-2Ac]^-$,575.1334 $[M-H-2Ac-146-132]^-$,443.8000 $[Aglycone-H]^-$	Spirostane steroidal saponin	[14]
35	5.53	+	+	623.1563	$C_{28}H_{32}O_{16}$	250, 342	Isorhamnetin rutinoside	605.1334, 314.0333, 300.0667	Flavonol	[37,65]
36	5.71	+	+	341.0995	$C_{19}H_{18}O_6$	296	Methylophiopogonanone A	308.9333, 265.1333, 213.1000, 178.9000	Homoisoflavanone	[68]
37	6.36	-	+	377.0069	$C_{19}H_{22}O_8$	-	methyl 4-[1,3-dihydroxy-1-(4-hydroxy-3-methoxyphenyl) propan-2-yl] oxy-3-methoxybenzoate	329.0667, 223.8333, 187.4000	Benzoic acid derivative	[38]
38	6.46	+	+	255.2303	$C_{15}H_{12}O_4$	267	Pinocembrine ((R)-5,7-dihydroxyflavanone)	210.8333, 192.8333, 192.8333, 164.8000	Flavanone	[38]
39	6.47	+	-	1099.282	$C_{53}H_{80}O_{24}$		Tetrahydroxy spirosta-diene-diacetyl deoxyhexoside dipentoside deoxyhexose	1099.2820 $[M-H]^-$,1057.3000$[M-Ac]^-$,737.0666$[M-146-$ 2 Ac -132-$]^-$,604.7333$[M-146-2Ac-$ 132 - 132$]^-$	Spirostane steroidal saponin	[14]
40	6.66	+	+	593.1458	$C_{27}H_{30}O_{15}$	265, 347	Kaempferol hexoside deoxyhexoside	284.9667, 254.9667, 223.0333, 216.6333, 182.3000	Flavonol	[38]

41	7.24	+	+	651.1877	$C_{31}H_{40}O_{15}$	272, 316	Martynoside	589.0334, 477.9000, 471.1000, 346.0000	Phenylpropanoid glycoside	[84]
42	7.66	+	+	953.4429	$C_{47}H_{70}O_{20}$	-	Tetrahydroxy spirosta-diene-diacetyldeoxyhexoside dipentoside	953.4429 $[M-H]^-$,910.2000 $[M-Ac]^-$,867.1000 $[M-H-2Ac]^-$, 457.4667 $[Aglycone-H]^-$	Spirostane steroidal saponin	[14]
43	8.44	+	+	611.2781	$C_{27}H_{31}O_{16}$	286	Eriodictyol dihexoside	593.1667, 468.6667, 284.9667	Flavanone	[61]
44	9.87	+	+	853.3217	$C_{43}H_{66}O_{17}$	-	Trihydroxy spirosta-diene-deoxyhexoside dipentoside	853.3217 $[M-H]^-$, 721.3000 $[M-H-132]^-$, 589.7333 $[M-H-132-132]^-$, 443.5000 $[Aglycone-H]^-$	Spirostane steroidal saponin	[14]
45	10.02	+	+	741.255	$C_{38}H_{62}O_{14}$	-	Trihydroxyspirostane hexoside pentoside	741.2550 $[M-H]^-$, 723.4000 $[M-H-H_2O]$, 581.0000 [M-H-162], 542.5334 $[M-H-162-2H_2O]^-$, 428.5667 $[M-H-162-132-H_2O]^-$	Spirostane steroidal saponin	[49]
46	10.38	+	+	331.2805	$C_{13}H_{16}O_{10}$	262, 376	Monogalloyl-hexoside	311.1333, 270.6667, 165.2667	gallotannin	[71]
47	11.16	+	+	371.1213	$C_{16}H_{20}O_{10}$	267, 298	Hydroxydihydrocaffeoylquinic acid	355.1000, 195.3000, 178.5333, 165.1333	Cinnamic acid derivative	[56]
48	11.39	+	+	299.0533	$C_{16}H_{12}O_6$	254, 295, 337	Isokaemferide (5,7,4`-trihydroxy-3-methoxyflavone)	281.0333 $[M-H-H_2O]^-$, 268.1667 $[M-CH_3O]^-$, 255.8667	Flavone	[21]
49	11.80	+	-	1075.4847	$C_{52}H_{84}O_{23}$	-	Dihydroxy methoxyfurost--diene deoxyhexoside trihexoside	1075.4847 $[M-H]^-$, 928.6667 $[M-H-146]^-$, 751.6000 $[M-H-2\ X\ 162]^-$, 604.6667 $[M-H-146-2\ X\ 162]^-$	Furostane steroidal saponins	[52]
50	11.86	+	+	869.4447	$C_{44}H_{70}O_{17}$	-	Hydroxyspirost-en deoxyhexoside pentoside hexoside	869.4447 $[M-H]^-$, 737.3000 $[M-H-132]^-$, 723.2666 $[M-H-146]^-$, 591.2000 $[M-H-132-146]^-$	Spirostane steroidal saponin	[11]
51	12.20	+	-	895.2334	$C_{45}H_{68}O_{18}$	-	Trihydroxy spirosta-diene acetyl deoxyhexoside dipentoside	941.4313 $[M+FA-H]^-$, 895.2334 $[M-H]^-$, 705.6667 $[M-H-Ac-146]^-$, 572.6000 $[M-H-Ac-146-132]^-$	Spirostane steroidal saponin	[14]
52	12.27	+	+	811.3682	$C_{40}H_{60}O_{17}$	-	Dihydroxypregna-5,16-dien-20-one deoxyhexoside pentoside acetyl hexoside	811.3682 $[M-H]^-$, 795.4000 $[M-H_2O]^-$, 769.1000 $[M-H-Ac]^-$, 679.2334 $[M-H-132]^-$, 533.1000 $[M-H-132-146]^-$	Pregnane steroidal saponin	[15]
53	12.61	-	+	297.0738	$C_{17}H_{14}O_5$	289	Dimethoxy hydroxyflavone	281.0667, 268.9333, 253.1000, 237.6000	Flavone	[37]

54	12.96	+	+	835.369	$C_{40}H_{68}O_{18}$	-	Hexahydroxy methoxyfurostane dihexoside	835.3690 $[M-H]^-$, 673.5000 $[M-H-162]^-$, 511.9667 $[M-H-162-162]^-$	Furostane steroidal saponins	[51]
55	13.89	+	-	255.2303	$C_{15}H_{12}O_4$	285	Trihydroxychalcone	238.8333, 226.0000, 211.5667, 186.8000	Chalcone	[37]
56	15.01	+	+	315.6990	$C_{13}H_{16}O_9$	280	Protocatechuic acid hexoside	296.8667, 271.0000, 152.8731, 109.0700	Benzoic acid derivative	[53]
57	15.85	+	+	353.1208	$C_{16}H_{18}O_9$	273,329	Chlorogenic acid	309.5000, 189.5667	Cinnamic acid derivative	[55]
58	15.85	+	+	301.0003	$C_{16}H_{14}O_6$	263	Hesperetin	282.9000, 273.0000, 239.0000, 195.0667, 167.1333, 125.1333	Flavonol	[37]
59	18.71	+	-	911.4200	$C_{45}H_{68}O_{19}$	-	Tetrahydroxy spirosta-diene acetyl deoxyhexoside dipentoside	911.4200 $[M-H]^-$, 869.4333 $[M-H-Ac]^-$, 851.4000 $[M-H-CH_3COOH]^-$, 591.3333 $[M-H-Ac-146-132]^-$	Spirostane steroidal saponin	[14]
60	18.78	+	+	315.0843	$C_{17}H_{16}O_6$	267	Dihydroxy-dimethoxyflavanone	300.0000, 285.0033, 270.1023, 225.1005, 165.0000	Flavanone	[37]
61	18.96	+	+	283.1887	$C_{16}H_{12}O_5$	265, 327	Acacetin	250.6333, 239.1667, 219.2333, 198.8667	Flavone	[37]
62	19.91	+	+	529.1360	$C_{26}H_{26}O_{12}$	-	Caffeoyl–feruloylquinic acid	486.9000, 349.0000, 220.5333	Cinnamic acid derivative	[57]
63	24.79	+	+	285.0741	$C_{15}H_{10}O_6$	265, 365	Kaempferol	279.0000, 269.9667, 239.0667, 178.8333, 164.9333	Flavonol	[37]
64	31.08	-	+	311.0896	$C_{13}H_{12}O_9$	265, 347	Caftaric acid	293.1667, 274.1667, 182.7333, 157.0333, 130.1333, 119.3333	Cinnamic acid derivative	[58]
65	34.19	+	+	429.2451	$C_{27}H_{42}O_4$	-	Ruscogenin	383.0667, 365.3333, 344.8000, 324.9667, 292.7667	Spirostane steroidal saponin	[44]
66	34.45	+	+	426.9193	$C_{27}H_{40}O_4$	-	Neoruscogenin	395.2666, 358.8000, 344.7000, 298.0000	Spirostane steroidal saponin	[44]

Table 2: List of steroidal saponins previously reported in literature and have similar MS data to the identified compounds in *S. trifasciata* extracts.

Peak No.	**Saponin**	**References**
1	(23S,24S)-spirosta-5,25(27)-diene-1β,3 β ,23,24-tetrol-1-O-{O-(2,3,4-O-triacetyl-α-L-rhmnopyranosyl)-(1→2)-O-[β-D-xylopyranosyl-(1→3)]-α-L-arabinopyranoside}24-O- β-D-glucopyranoside	[14]
2	(23S,24S)-spirosta-5,25(27)-diene-1β,3 β ,23,24-tetrol-1-O-{O-(2,3,4-O-triacetyl-α-L-rhmnopyranosyl)-(1→2)-O-[β-D-xylopyranosyl-(1→3)]-α-L-arabinopyranoside}24-O- rhamnopyranoside or fucopyranoside	[14]
5	(23S,24S)-Spirosta-5,25(27)-dien-1β,3β,23,24-tetrol 1-O-[4-O-acetyl-α-L-rhamnopyranosyl-(1→2)-,α-L-arabinopyranoside}-24-O-β-D-fucopyrnoside (Namonin D)	[48]
7	6,(24S,25S)-5α-Spirostane-2α,3β,5,6β,24-pentol 2-O-{β-D-glucopyranoside-24-O-β-D-glucopyranosyl-(1→2)-β-D-glucopyranoside	[50]
8	1β,3β- dihydroxypregna-5,16-dien-20-one 1-O-{O-α-L-rhamnopranosyl-(1→2)-O-[β-D-xylopyranosyl-(1→3)]-β-D-glucopyranoside}	[15]
10	Neoruscogenin 1-O-{α-L-rhamnopyranosyl-(1→2)-[β-D-xylopyranosyl-(1→3)]-α-L-arabinopyranoside}	[45]
29	26-[(β-D-glucopyranosyl) oxy]-3β-hydroxy-22α-methoxy-(25S)-furost-5-en-1β-yl-O-α-L-rhamnopyranosyl-(1→2)-O-[β-D-xylopyranosyl-(1→3)]-β-D-glucopyranoside (trifasciatoside F).	[11]
33	1 β,3 β -Dihydroxypregna-5,16-dien-20-one 1-O- {α -L-rhamnopyranosyl-(1→2)- [β -D-xylopyranosyl-(1→3)]-α -L-arabinopyranoside}	[15]
34	23S)-spirosta-5,25(27)-diene-1 β,3 β,23-triol-1-O-{O-(2,3-O-diacetyl-α-L-rhamnopyranosyl) -(1→2)-O[β-D-xylopyranosyl-(1→3)]-α-L-arabinopyranoside}	[14]
39	(23S,24S)-spirosta-5,25(27)-diene-1β,3 β ,23,24-tetrol-1-O-{O-(2,3-O-diacetyl-α-L-rhmnopyranosyl)-(1→2)-O-[β-D-xylopyranosyl-(1→3)]-α-L-arabinopyranoside}24-O- β-D-fucopyranoside	[14]
42	(23S,24S)-spirosta-5,25(27)-diene-1β,3 β ,23,24-tetrol-1-O-{O-(2,3-O-diacetyl-α-L-rhamnopyranosyl) -(1→2)-O-[β-D-xylopyranosyl-(1→3)]-α-L-arabinopyranoside}	[14]
44	(23S)-spirosta-5,25(27)-diene- β,3 β,23-triol-1-O-{O-α-L-rhamnopyranosyl-(1→2)-O-[β-D-xylopyranosyl-(1→3)]-α-L-arabinopyranoside}	[14]
45	Convallagenin A 3-O-[β-D-glucopyranosyl-(1→2)-α-L-arabinopyranoside] (Glucoconvallasaponin A)	[49]
49	(23S,25R)-23-Methoxyfurost-5,20(22)-diene 3,26-diol 3-O-{ α -L-rhamnopyranosyl-(1→2)-[β -D-glucopyranosyl-(1→3)- β -D-glucopyranoside}-26-O- β -D-glucopyranoside (Dioscoreside E)	[52]
50	(25R)-3β-hydroxyspirost-5-en-1β-yl-O-α-L-rhamnopyranosyl-(1→2)-O-[β-D-xylopyranosyl (1→3)]-β-D-glucopyranoside (Trifasciatoside C)	[11]
51	(23S)-spirosta-5,25(27)-diene-1 β,3 β,23-triol-1-O-{O-(4-O-acetyl-α-L-rhamnopyranosyl)-(1→2)-O-[β-D-xylopyranosyl-(1→3)]-α-L-arabinopyranoside}	[14]
52	1β,3β- dihydroxypregna-5,16-dien-20-one 1-O-{O-α-L-rhamnopranosyl-(1→2)-O-[β-D-xylopyranosyl-(1→3)]-6-O-acetyl-β-D-glucopyranoside}	[15]
54	1β,2β,3β,4β,5β,26-Hexahydroxy-22ε-methoxyfurostane 3,26-bis-O-β-D-glucopyranoside	[51]
59	(23S,24S)-spirosta-5,25(27)-diene-1β,3 β ,23,24-tetrol-1-O-{O-(4-O-acetyl-α-L-rhmnopyranosyl)- (1→2)-O- [β-D-xylopyranosyl-(1→3)]-α-L-arabinopyranoside}	[14]
65	Ruscogenin	[44]
66	Neoruscogenin	[44]

Table 3: Primer sequences for RT-q PCR.

Gene	**Primer sequence (5′-3′)**		**Accession #**	**Product (bp)**
Nrf2	F	CACATCCAGACAGACACCAGT	XM_006234398.3	121
	R	CTACAAATGGGAATGTCTCTGC		
Keap1	F	AACTCGGCAGAATGTTACTACCC	NM_017000.3	190
	R	CTACGAAAGTCCAGGTCTCTGTCTC		
NQO1	F	TCAAGAGGAGCAGAAAAAGAACAAG	XM_006242591.3	162
	R	CTGAAAGCAAGCCAGGCAAAC		
HO-1	F	ACAGGGTGACAGAAGAGGCTAA	NM_012580.2	107
	R	CTGTGAGGGACTCTGGTCTTTG		
β-actin	F	ATGGTGGGTATGGGTCAG	NM_031144.3	97
	R	CAATGCCGTGTTCAATGG		

Nrf2, nuclear factor erythroid 2-related factor 2; Keap-1, kelch-like epichlorohydrin-associated protein 1; NQO1, NAD(P)H dehydrogenase [quinone] 1; HO-1, haeme oxygenase-1.

Table 4: Effect of *S. trifasciata* hort ex. Prain leaves' (StLE) and roots' (StRE) extracts on hepatic GSH and MDA contents.

Groups	GSH (µmol/g tissue)	MDA (nmol/g tissue)
Control group	55.5±1.94[b]	3.0±0.12[b]
TAA group	6.7 ±0.32[a]	25.8±1.35[a]
StLE (200 mg/kg)	25.5±0.73[ab]	12.4±0.23[ab]
StLE (100 mg/kg)	14.9±0.50 [ab]	17.5±0.69 [ab]
StRE (200 mg/kg)	46.1±1.18 [ab]	6.5±0.17 [ab]
StRE (100 mg/kg)	36.7±1.42 [ab]	9.7±0.33 [ab]
Silymarin	40.1±1.19 [ab]	7.2±0.27 [ab]

Values are expressed as mean ± SEM; [a]$P \leq 0.05$ compared with that normal control group and [b]$P \leq 0.05$ compared with TAA group.

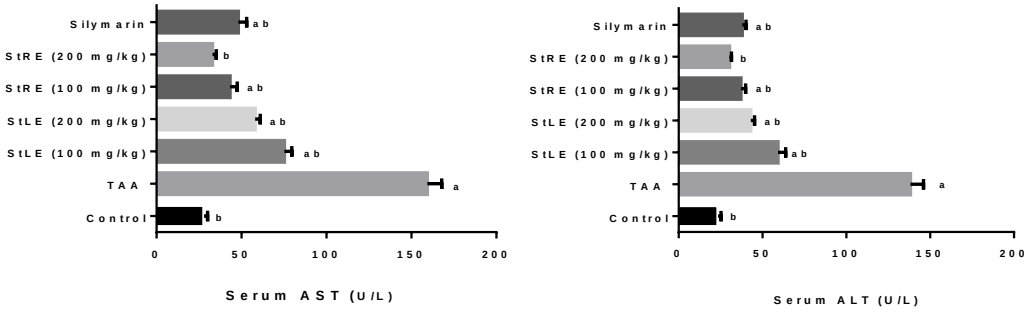

Figure 3: Effect *of S. trifasciata* hort ex. Prain leaves' (StLE) and roots' (StRE) extracts on serum AST and ALT levels.

Values are expressed as mean±SEM; [a]$P \leq 0.05$ compared with that control group and [b]$P \leq 0.05$ compared with TAA group.

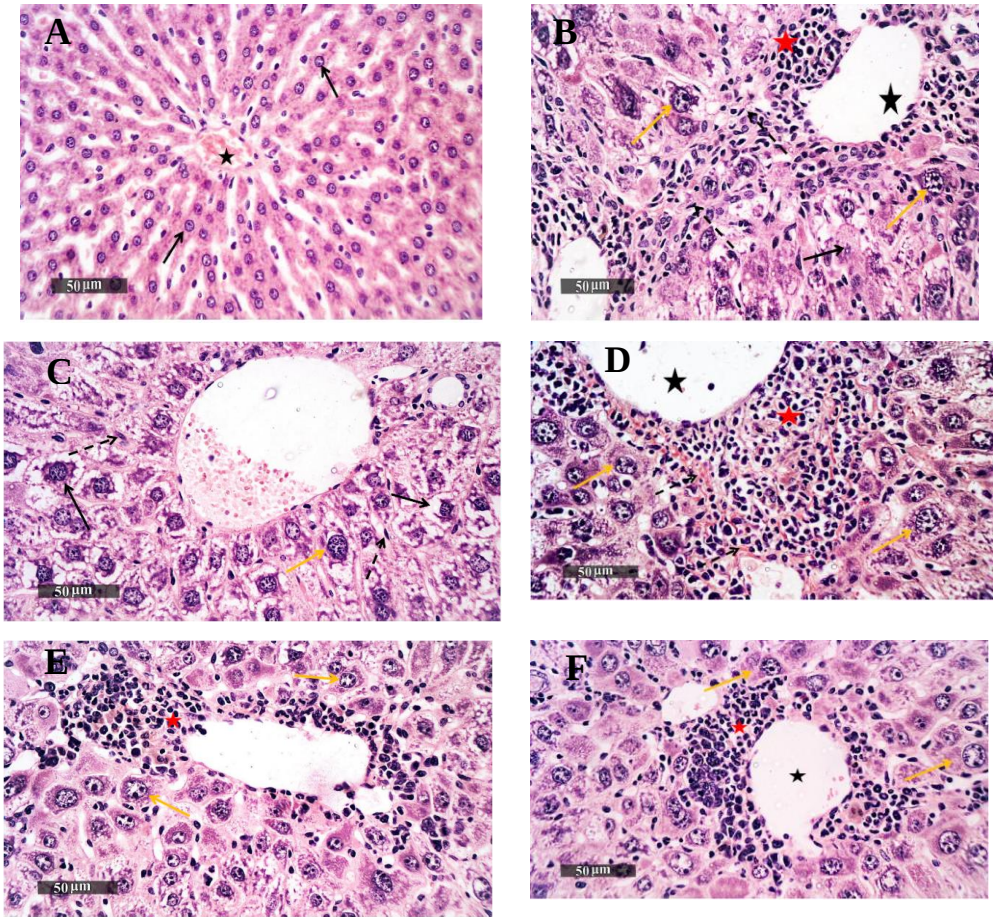

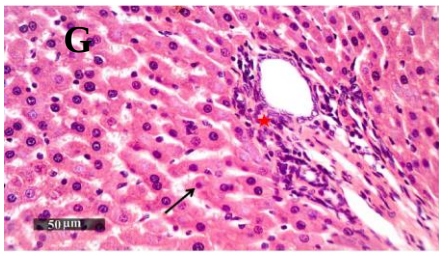

Figure 4: (A) Liver (H&E) of rat from control group demonstrated normal histological features of hepatic parenchyma with many apparent intact hepatocytes allover hepatic lobules. **(B)** Liver of a rat from TAA-group showed sever necrotic and degenerative hepatocellular records (black arrow) with many figures of hepatocytomegaly (yellow arrow) accompanied with many dilated and congested blood vessels (black star). Sever periportal inflammatory cells infiltrates (red star). **(C)** Liver section of a rat from StLE (200 mg/kg) group showed significant reduction of periportal inflammatory cells infiltrates records with mild occasional records of hepatocytomegaly (yellow arrow). However; sever vacuolar degenerative changes with cytoplasmic reticulation (black arrow) as well as moderate persistence of fibroblastic activity was observed (dashed arrow) with mild pesudolobulation. **(D)** Liver section of a rat from StLE (100 mg/kg) group showed degenerative hepatocytes (black arrow) with some hepatocytomegaly (yellow arrow) accompanied with some dilated and congested blood vessels (black star) and Sever periportal inflammatory cells infiltrates (red star). **(E)** Liver of a rat from StRE (200 mg/kg) group showed moderate persistence of periportal collagen fibers with activated fibroblasts (dashed arrow) and mild interlobular bridging. Moderate perivascular inflammatory cell infiltrates (red star) were observed accompanied with many aspects of hepatocytomegaly (yellow arrow) as well as degenerative changes. **(F)** Liver of a rat from StRE (100 mg/kg) group showed the same records as StLE 200 group with more abundant dilated and congested blood vessels (star). **(G)** liver section of a rat from silymarin group showed almost well-organized apparent intact hepatocytes with minimal degenerative changes records (arrow). However; mild periportal persistence of inflammatory cells infiltrates as well as collagen fibrous tissue were observed (red star).

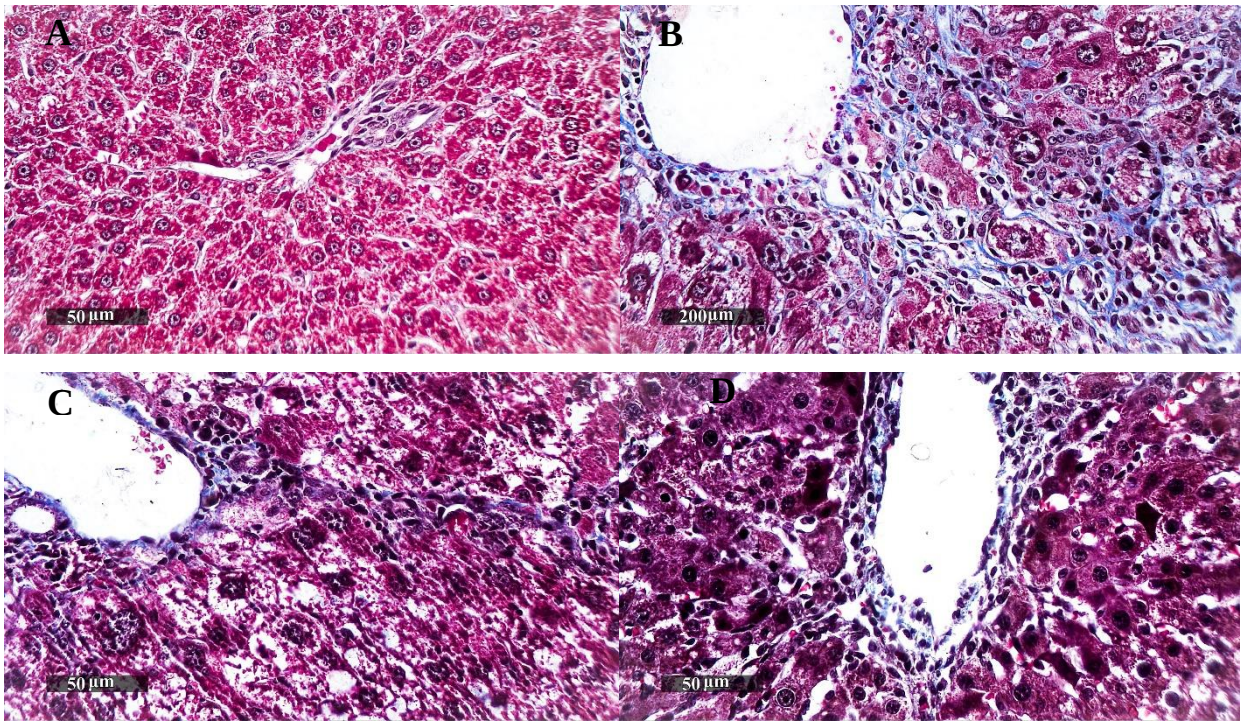

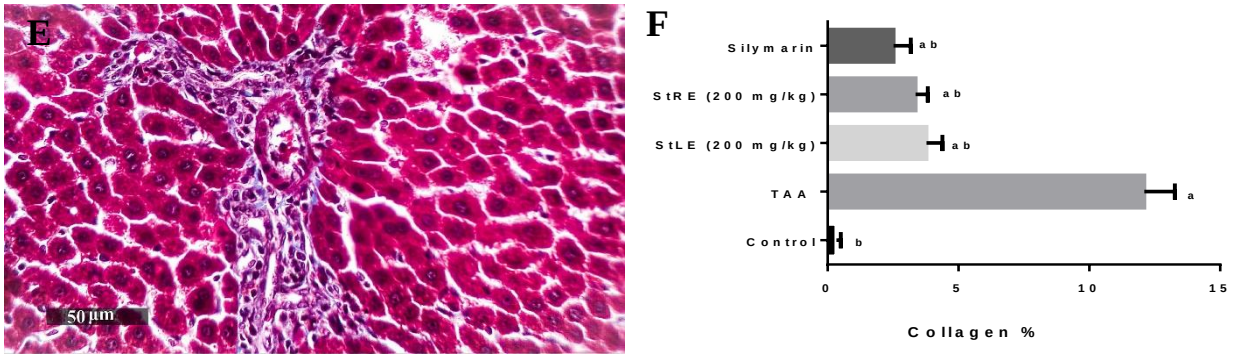

Figure 5: Liver sections stained with Masson's trichrome stain of rats from **(A)** control group. (**B)** TAA-group. (**C)** StLE (200 mg/kg) group. **(D)** StRE (200 mg/kg) group. **(E)** silymarin group.

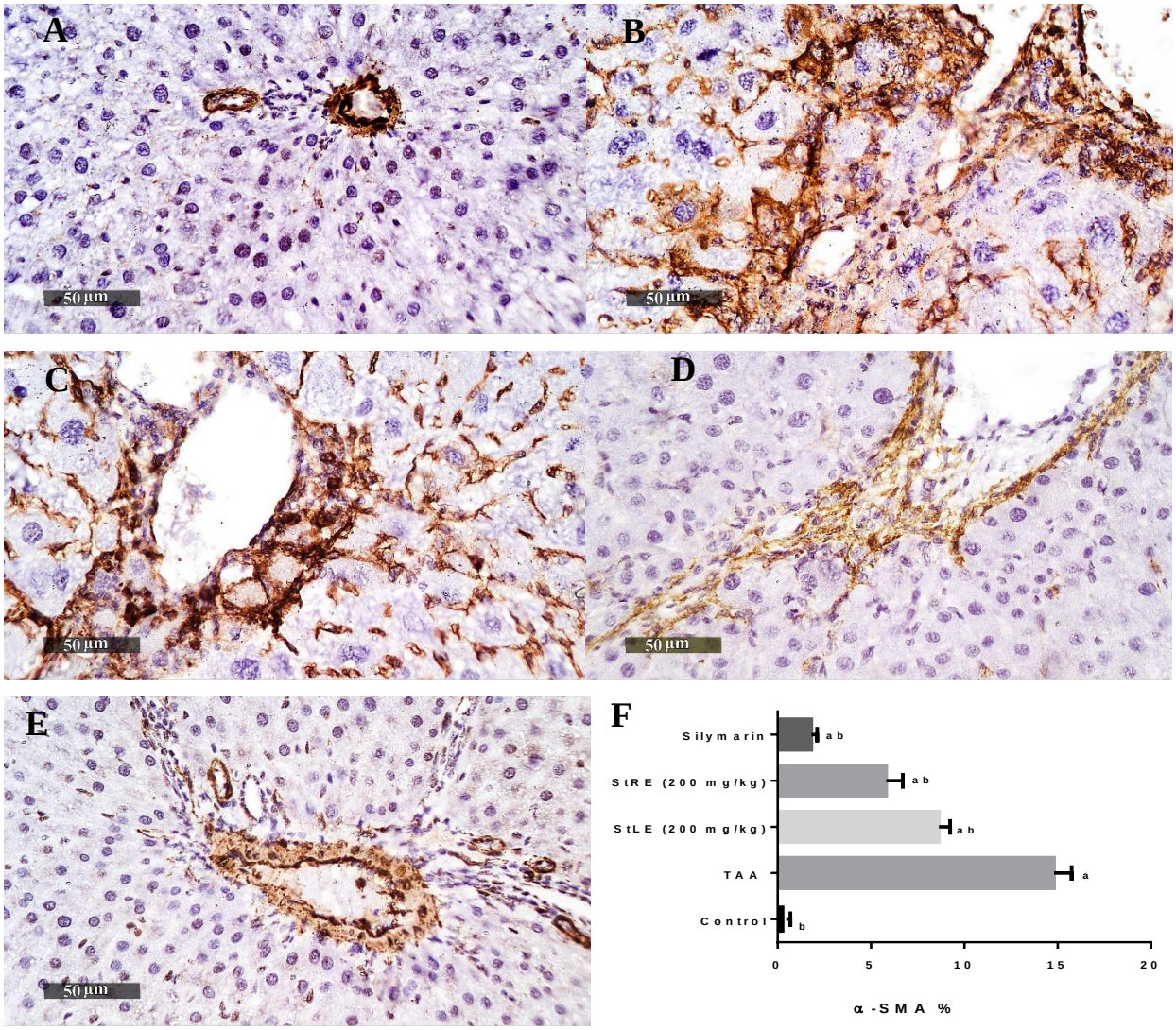

Figure 6: Immunohistochemical analysis of α-SMA in liver sections of rats from **(A)** control group. (**B)** TAA-group. (**C)** StLE (200 mg/kg) group. **(D)** StRE (200 mg/kg) group. **(E)** silymarin group.

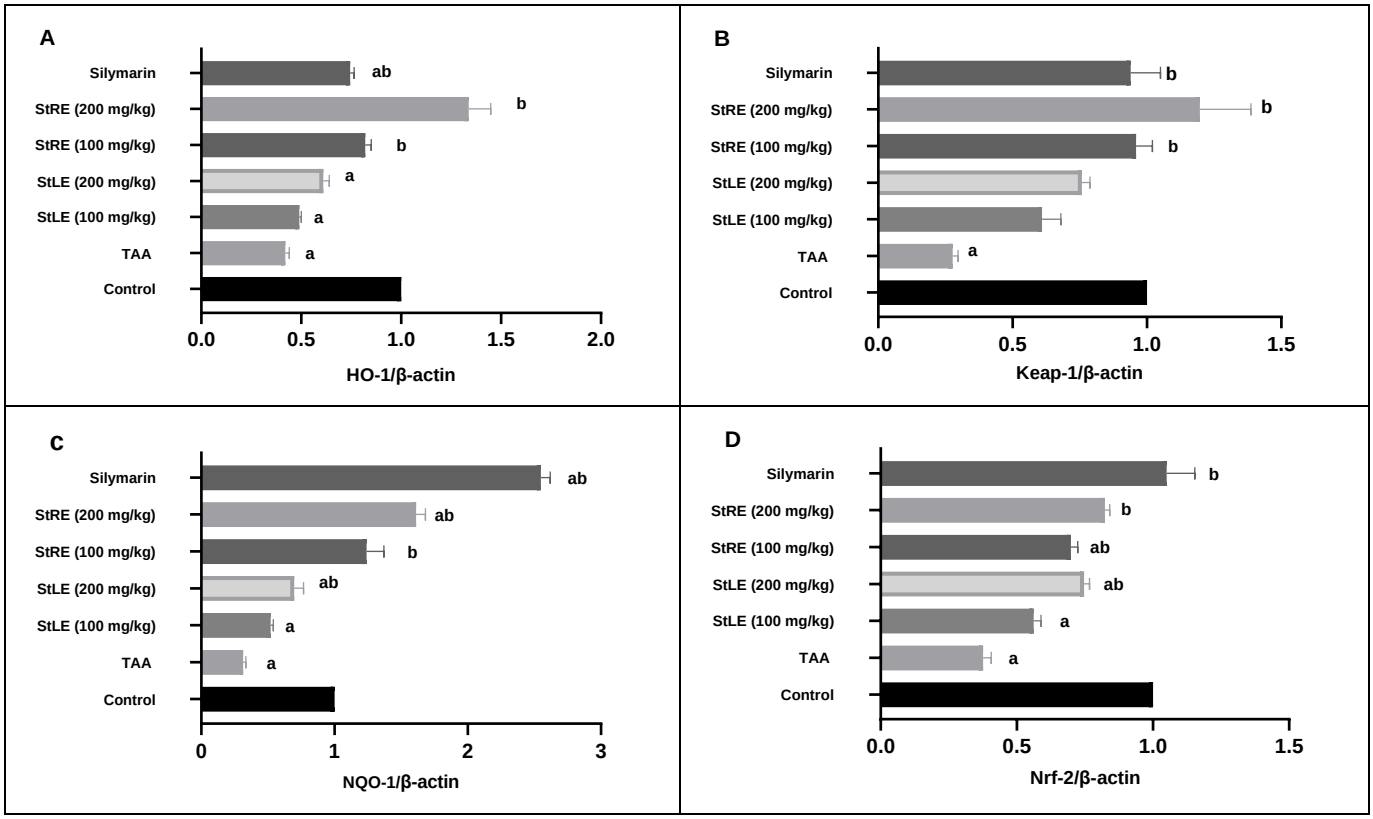

Figure 7: Effects of *S. trifasciata* hort ex. Prain leave extract (StLE) and roots extract (StRE) on gene expression of HO-1 (A), Keap-1 (B), NQO-1 (C), and Nrf-2 (D) in liver tissue of TAA-induced hepatic fibrosis rat model. The relative mRNA transcript levels of the target genes are represented as fold changes over that of the normal group after normalization to the housekeeping gene β-actin using the $2^{-\Delta\Delta Ct}$ method. values are expressed as mean±SEM. Statistical analysis was carried out using one-way ANOVA followed by Tukey's multiple comparison test; [a] vs control and [b] vs TAA group at $p \leq 0.05$.

3.1.2.4. Coumarins

Two peaks were detected in both extracts and suggested to be coumarin derivatives. Peaks 22 and 32 produced the molecular ions $[M-H]^-$ at m/z 325 and 421, respectively. According to the MassBank of North America (MoNA) [38] and literature data [70], they were tentatively assigned as p-coumaric acid-O-glucoside and 6-((6-ethyl-4-hydroxy-5-methyl-2-oxo-2H-pyran-3-yl) methyl)-5,7-dihydroxy-2-phenylchroman-4-one, respectively.

3.1.2.5. Gallic Acid Derivatives

Peak 46 along with its molecular ion $[M-H]^-$ at m/z 331 has been detected in both extracts. It was tentatively assigned as monogalloyl-hexoside based on the MS/MS fragments at m/z 311, 270 and 165. [71]. Gallic acid was previously identified in other *Sansevieria* species, *S. roxburghiana* [72].

Plant phenolics incorporate simple phenols, phenolic acids, coumarins, lignans, flavonoids, stilbenoids and gallic acid derivatives, are well known for their antioxidant activity as well as other health benefits such as antimicrobial, anticancer, anti-inflammatory and anti-mutagenic activities [73]. They act as natural scavengers for toxic elements and, thus, reduce the risk of various hepatic disorders, especially hepatocellular tumors in humans [74]. As phenolics influence hepatotoxicity through altered mechanisms such as protection against oxidative damages, stabilization of cell membrane networks and inhibition of the evolution and expression of inflammatory cytokines as tumor necrosis factor-alpha (TNF-α), Transforming Growth Factor beta (TGF-β) and diversity of interleukins (IL-6, IL-2, IL-8) [75].

3.1.3. Terpenoids

Four terpenoid derivatives were detected in both extracts. Peaks 6, 14, 15 and 19 detected at 2.68, 3.44,

3.53 and 3.83 min. possessed the molecular ions $[M-H]^-$ at m/z 345, 511, 457 and 247, respectively. According to MS/MS fragments, they were tentatively assigned as, aucubin, picroside п, lucidenic acid and pechueloic acid, respectively [38,76]. Terpenoids were previously reported in *S. trifasciata* [24].

Terpenoids are known to exhibit several biological actions such as antioxidant, anti-inflammatory, cytotoxic and hepatoprotective activities. In particular, pechueloic acid has cytotoxic activity and antiviral activity against influenza virus [77,78]. Aucubin, picroside ii, lucidenic acid and paeoniflorin possess significant hepatoprotective activity [79–82]

3.1.4. Sugars

Peak 3 detected in both extracts, showed the molecular ion $[M-H]^-$ at m/z 503, as well as its typical fragments at m/z 341, 323, 221 and 179 that suggested it was identified as raffinose [37].

3.1.5. Other Compounds

Peak 16 with the molecular ion $[M-H]^-$ at m/z 585 and its daughter fragments at m/z 423, 379 and 263, was detected in both extracts and characterized as hydroxyhispidin dihexoside glucoside [83]. Peak 41 with the molecular ion $[M-H]^-$ at m/z 651 and its daughter fragments at m/z 589, 477, 471 and 346, was detected in both extracts and characterized as martynoside [84].

3.2. Hepatoprotective Effect

In our present research, TAA-induced liver fibrosis in rats has been setteled biochemically and confirmed through the histopathological findings. Serum levels of ALT and AST were significantly elevated in TAA group, as shown in figure 3. This elevation may be elucidated due to liver cell destruction or variations in the membrane permeability proposing their leakage from harmed hepatocytes into the blood [85]. Administration of the two parts of *Sansevieria trifasciata* in the current study significantly improved the liver function parameters in comparison to TAA group and the restorative action has been more prominent in StRE groups than StLE groups, particularly StRE at a dose of 200 mg/kg. Additionally, silymarin treated rats (100 mg/kg/day) showed a significant decrease in serum levels of AST and ALT as compared to TAA group.

Furthermore, the oxidative stress induced by TAA was evidenced by the reduction in the normal liver GSH content in addition to an increase in MDA content as shown in TAA group (Table 4). Notably, depletion of GSH is greatly related to the lipid peroxidation which is documented as a probable cell injury mechanism. Besides, GSH plays a key protective role in many mammalian tissues as a scavenger of free radicals that combines with non-protein thiols to abolish free radical toxicity [86]. Administering StLE and StRE orally at doses of 200 and 100 mg/kg/day, significantly counteracted the oxidative stress induced by TAA that evidenced by a significant increase in liver GSH content and a marked decrease in MDA levels, compared to TAA group. The most pronounced effect was shown in StRE group at a dose of 200 mg/kg/day. Histopathological examination of liver sections was depicted in figure 4. Control rats revealed normal histological features of hepatic parenchyma with many apparent intact hepatocytes allover hepatic lobules. While liver of rats from TAA-group showed severe necrotic and degenerative hepatocellular records with evidence of hepatocytomegaly and many dilated and congested blood vessels. Moreover, severe periportal inflammatory cells infiltrates were detected. Treatment of rats with StLE demonstrated significant reduction of periportal inflammatory cells infiltrates records with mild occasional records of hepatocytomegaly. Whereas; severe vacuolar degenerative changes with cytoplasmic reticulation as well as moderate persistence of fibroblastic activity was observed, accompanied with mild pesudolobulation. On the other hand, treatment of rats with StRE showed moderate persistence of periportal collagen fibers with activated fibroblasts and mild interlobular bridging. Moderate perivascular inflammatory cell infiltrates were observed accompanied with many aspects of hepatocytomegaly. Silymarin treated rats showed almost well-organized apparent intact hepatocytes with minimal degenerative changes records, with mild periportal persistence of inflammatory cells infiltrates as well as collagen fibrous tissue was observed. Additionally, liver sections stained with Masson's trichrome stain are demonstrated in figure (5). This stain specifically stains the collagen in blue denoting fibrous tissue. Quantitative analysis (Figure 5-F) revealed strongly blue in TTA group, while in groups treated with either StLE or StRE are showing diminished blue-stained collagen fibers. Additionally, as demonstrated in figure 6, immunohistochemical examination of α-SMA in liver sections showed strong immunostaining in TAA group. In this context, administration of TAA progress hepatic fibrosis and activation of myofibroblasts as demonstrated by increasing the expression of α-SMA [85]. Remarkably, *S. trifasciata* extracts (StLE and StRE) significantly reduced the expression of α-SMA compared to TAA group, suggesting their potential antifibrotic activity.

3.3. Effects on Nrf2 Signaling and its Downstream Genes in TAA-Induced Liver Fibrosis

To further explore the molecular mechanism underlying the antioxidant efficacy of StLE and StRE, our study focused on Keap1-Nrf2/ARE signaling. The

Nrf2/ARE pathway plays a vital role in defending against oxidative damage and inflammation by regulating the antioxidant enzymes system and maintaining the cellular redox homeostasis [87]. Nrf2 is a transcription factor that induces the expression of more than 90% of antioxidative genes to initiate a response to oxidative stress [88]. Many studies on various models of hepatic injuries have reported that activation of Keap1–Nrf2 pathway could alleviate oxidative liver damage. Thus, dysregulation of Nrf2 leads to substantial enrichment of reactive oxygen spices (ROS) and thereby has been correlated with the progression of chronic inflammatory diseases [89,90]. Nrf2 is a chief regulator of cellular oxidative stress, and in case of homeostatic circumstances, binds to Kelch-like ECH-associated protein 1 (Keap1), thus it is latterly degraded by-way-of the proteasome system or stored in cytoplasm. If oxidative stress exists, Nrf2 transfers to the nucleus and binds specifically to antioxidant response elements (AREs) [91]. Activation of Nrf2-ARE signaling can induce the transcription of various downstream antioxidant genes, as glutathione-S-transferase, HO-1, and NQO1 [92,93]. As shown in figure (7). qRT-PCR analysis showed that hepatic mRNA levels of Nrf2, HO-1, NQO-1 and Keap-1 were significantly decreased ($P \leq 0.05$) in TAA group compared to the normal control. Interestingly, StRE at the two studied doses (100 and 200 mg/kg) as well as silymarin effectively reverts the TAA effects on the expression of Nrf2, HO-1, NQO-1 and Keap-1. Such findings suggest that StRE may protect against TAA-induced liver injury through the upregulation of Nrf2 signaling. On the other hand, StLE (100 mg/kg) treated groups showed slightly increased expression levels of Nrf2, HO-1, NQO-1 and Keap-1 but the differences were not significant ($P>0.05$) compared to TAA group. Meanwhile, StLE treated group at a dose of 200 mg/kg exhibited a remarkable elevation in both the Nrf2 and NQO-1 expression. The prominent hepatoprotective activity of StRE may be attributed to certain phenolic constituents which were not detected in StLE as previously mentioned. Previous studies stated the fact that phenolic compounds contain a hydroxyl group which contributes for free radical scavenging activity [94]. A close correlation between phenolic content and antioxidant activity was highlighted in the study of [29].

4. Conclusions

This study represents the first proposal of the metabolomic profiles of *Sansevieria trifasciata* hort ex. Prain leaves and roots using HPLC-PAD-MS/MS. The HPLC phytoconstituents profiles give a deeper insight into the chemistry of *Sansevieria trifasciata*, clarify the difference between leaves and roots constituents, and explain their rely on the plant bioactivities. The identified phytoconstituents were mainly steroidal saponins, phenolics and terpenoids. Sixty-one compounds were tentatively identified in StLE and fifty-nine compounds in StRE. The common compounds in both extracts were fifty-four compounds. Seven compounds were only characterized in StLE. Five compounds were only found in StRE.

Herein, we found that *Sansevieria trifasciata* inhibited liver fibrosis induced by TAA in rats by prompting the expression of Nrf2 and its downstream antioxidant enzymes in a rat model of TAA-induced hepatic fibrosis. Both extracts of *S. trifasciata* leaves and roots revealed hepatoprotective activity, which was more prominent in StRE than StLE treated groups. These findings were supported by the histological and molecular evidences. This supports the use of *Sansevieria trifasciata* in traditional health care for managing liver problems.

Conflicts of interest

There are no conflicts to declare.

Formatting of Funding Sources

This study was funded by the National Research Centre (Project number: 12060109).

Acknowledgement

The authors wish to acknowledge the National Research Centre for financial support (Project number: 12060109) and Dr. Stephen J. Eyles, Director of UMass-Amherst Mass Spectrometry Center, University of Massachusetts, Maryland, USA, for helping in HPLC-MS analysis. The authors gratefully acknowledge Dr. Mohamed A. Khattab for his assistance with the histopathological examination.

References

1. Trautwein C., Friedman S.L., Schuppan D. and Pinzani M, Hepatic fibrosis: Concept to treatment. *J. Hepatol.*, **62**(1), S15-S24 (2015).
2. Argemi J. and Bataller R., Identifying new epigenetic drivers of liver fibrosis. *Cell Mol. Gastroenterol. Hepatol*., **7**, 237–238 (2019).
3. Lu P., Yan M., He L., Li J., Ji Y. and Ji J., Crosstalk between epigenetic modulations in valproic acid deactivated hepatic stellate cells: an integrated protein and mirna profiling study. *Int. J. Biol. Sci*., **15**, 93–104 (2019).
4. Tipoe G.L., Leung T.M., Liong E.C., Lau T.Y.H., Fung M.L. and Nanji A.A., Epigallocatechin-3-gallate (EGCG) reduces liver inflammation,

oxidative stress and fibrosis in carbon tetrachloride (CCl4)-induced liver injury in mice. *Toxicology*, **273** (1-3), 45–52 (2010).
5. Ghatak S., Biswas A., Dhali G.K., Chowdhury A., Boyer J.L. and Santra A., Oxidative stress and hepatic stellate cell activation are key events in arsenic induced liver fibrosis in mice. *Toxicol. Appl. Pharmacol*., **251**, 59–69(2011).
6. Wang W., Guan C., Sun X., Zhao Z., Li J., Fu X., Qiu Y., Huang M., Jing J. and Huang Z., Tanshinone IIA protects against acetaminophen-induced hepatotoxicity via activating the Nrf2 pathway. *Phytomedicine*, **23** (6), 589–596 (2016).
7. Jiang Y., Wang Y., Tan H., Yu T., Fan X., Chen P., Zheng H., Huang M. and Bi H.C., Schisandrol B protects against acetaminophen-induced acute hepatotoxicity in mice via activation of the NRF2/ARE signaling pathway. *Acta Pharmacol. Sin*., **37** (3), 382–389 (2016).
8. Aleksunes L.M., Slitt A.L., Maher J.M., Augustine L.M., Goedken M.J., Chan J.Y., Cherrington N.J., Klaassen C.D. and Manautou J.E., Induction of Mrp3 and Mrp4 transporters during acetaminophen hepatotoxicity is dependent on Nrf2. *Toxicol. Appl. Pharmacol*., **226** (1), 74–83 (2008).
9. Ilyas U., Katare D.P., Aeri V. and Naseef P.P., A review on hepatoprotective and immunomodulatory herbal plants. *Pharmacogn. Rev*., **10**, 66–70 (2016).
10. Lu P-L. and Morden C.W. Phylogenetic relationships among Dracaenoid genera (Asparagaceae: Nolinoideae) inferred from Chloroplast DNA Loci. *Syst. Bot*., **39** (1), 90–104 (2014).
11. Teponno R.B., Tanaka C., Jie B., Tapondjou L.A. and Miyamoto T., Trifasciatosides A–J, steroidal saponins from *Sansevieria trifasciata*. *Chem. Pharm. Bull. (Tokyo)*, **64** (9), 1347-1355 (2016).
12. Morton J.F., Atlas of medicinal plants of middle America: Bahamas to Yucatan, First Edition, Charles C Thomas Pub Ltd, Florida, USA, p. 90–93 (1981).
13. González A.G., Freire R., García-Estrada M.G., Salazar J.A. and Suárez E., New sources of steroid sapogenins—XIV : 25S-ruscogenin and sansevierigenin, two new spirostan sapogenins from *Sansevieria trifasciata*. *Tetrahedron*, **28** (5), 1289–1297 (1972).
14. Mimaki Y., Inoue T., Kuroda M. and Sashida Y., Steroidal saponins from *Sansevieria trifasciata*. *Phytochemistry*, **43** (6), 1325–1331 (1996).
15. Mimaki Y., Inoue T., Kuroda M. and Sashida Y. Pregnane glycosides from *Sansevieria trifasciata*. *Phytochemistry*, **44** (1), 107–111 (1997).
16. Tchegnitegni B.T., Teponno R.B., Jenett-Siems K., Melzig M.F., Miyamoto T. and Tapondjou L.A., A dihydrochalcone derivative and further steroidal saponins from *Sansevieria trifasciata* Prain. *Zeitschrift fur Naturforsch - Sect C J. Biosci.*, **72** (11-12), 477–482 (2017).
17. Tchegnitegni B.T., Teponno R.B., Tanaka C., Gabriel A.F., Tapondjou L.A. and Miyamoto T., Sappanin-type homoisoflavonoids from *Sansevieria trifasciata* Prain. *Phytochem. Lett*., **12**, 262–266 (2015).
18. Gamboa-Angulo M.M., Reyes-López J. and Peña-Rodríguez L.M., A natural pregnane from *Sansevieria hyacinthoides*. *Phytochemistry*, **43** (5), 1079–1081 (1996).
19. Da Silva Antunes A., Da Silva B.P., Parente J.P. and Valente A.P.. A new bioactive steroidal saponin from *Sansevieria cylindrica*. *Phyther. Res*., **17** (2), 179–182 (2003).
20. Pettit G.R., Zhang Q., Pinilla V., Hoffmann H., Knight J.C., Doubek D.L., Chapuis J-C, Pettit R.K. and Schmidt, J.M., Antineoplastic agents. 534. Isolation and structure of sansevistatins 1 and 2 from the African *Sansevieria ehrenbergii*. *J. Nat. Prod*., **68** (5), 729–733 (2005).
21. Sultana N., Rahman M.M., Ahmed S., Akter S., Haque M.M., Parveen S. and Moeiz, S., Antimicrobial Compounds from the Rihzomes of *Sansevieria hyacinthoides*. Bangladesh J. Sci. Ind. Res., 46 (3), 329–332 (2011).
22. Raslan M.A., Melek F.R., Said A.A., Elshamy A.I., Umeyama A. and Mounier M.M., New cytotoxic dihydrochalcone and steroidal saponins from the aerial parts of *Sansevieria cylindrica* Bojer ex Hook. *Phytochem. Lett.*, **22**, 39–43 (2017).
23. Said A., Aboutabl E.A., Melek F.R., Abdel Jaleel G.A.R. and Raslan M.A., Steroidal saponins and homoisoflavanone from the aerial parts of *Sansevieria cylindrica* Bojer ex Hook. *Phytochem. Lett*., **12**, 113–118 (2015).
24. Sunilson J.A., Jayaraj P., Varatharajan R., Thomas J., James J. and Muthappan M., Analgesic and antipyretic effects of *Sansevieria trifasciata* leaves. *African J. Tradit. Complement. Altern. Med*., **6**, 529–533 (2009).
25. Qomariyah N., Sarto M. and Pratiwi R., Antidiabetic effects of a decoction of leaves of *Sansevieria trifasciata* in alloxan-induced diabetic white rats (*Rattus norvegicus* L.). *ITB J. Sci.*, **44A** (4), 308–316 (2012).
26. Andhare R.N., Raut M.K. and Naik S.R., Evaluation of antiallergic and anti-anaphylactic activity of ethanolic extract of *Sanseveiria trifasciata* leaves (EEST) in rodents. *J. Ethnopharmacol*. **142** (3), 627–633 (2012).
27. Sikder M.A.A., Siddique A.B., Nawshad Hossian A.K.M., Kowser Miah M., Kaisar M.A. and Rashid M.A., Evaluation of thrombolytic activity

of four Bangladeshi medicinal plants, as a possible renewable source for thrombolytic compounds. *J. Pharm. Nutr. Sci*., **1**, 4–8 (2011).
28. Al-Fatimi M., Wurster M., Schröder G. and Lindequist U., Antioxidant, antimicrobial and cytotoxic activities of selected medicinal plants from Yemen. *J. Ethnopharmacol*., **111** (3), 657–666 (2007).
29. Philip D., Kaleena P.K. and Valivittan K., Antioxidant potential of *Sansevieria roxburghiana* Schult. and Schult. f. Asian *J. Pharm. Clin. Res*., **5** (3), 166–169 (2012).
30. Moshi M.J., Mbwambo Z.H., Nondo R.S.O, Masimba P.J., Kamuhabwa A., Kapingu M.C., Thomas P. and Richardet M., Evaluation of ethnomedical claims and brine shrimp toxicity of some plants used in Tanzania as traditional medicines. *African J. Tradit. Complement. Altern. Med*., **3** (3), 48–58 (2006).
31. Haldar P.K., Kar B., Bhattacharya S., Bala A. and Kumar S.R.B., Antidiabetic activity and modulation of antioxidant status by *Sansevieria roxburghiana* rhizome in streptozotocin-induced diabetic rats. *Diabetol. Croat*., **39** (4), 115–123 (2010).
32. Said A., Aboutabl E.A., El Awdan S.A. and Raslan M.A., Proximate analysis, phytochemical screening, and bioactivities evaluation of *Cissus rotundifolia* (Forssk.) Vahl. (Fam. Vitaceae) and *Sansevieria cylindrica* Bojer ex Hook. (Fam. Dracaenaceae) growing in Egypt. Egypt Pharm. J., 14 (3), 180-186 (2015).
33. Ftahy M.M., Latif N.S.A., Alalkamy E.F., El-Batrawi F.A., Galal A.H. and Khatab H.M., Antifibrotic potential of a selective COX-2 inhibitor (celecoxib) on liver fibrosis in rats. *Comp. Clin. Path*., **22**, 425–430 (2013).
34. Culling C.F.A. Handbook of histopathological and histochemical techniques, Third edition, Butterworth & Co. (Publishers) Ltd, Elsevier, UK (1974).
35. Mansour D.F., Nada S.A., El-Denshary E.S., Omara E.A., Asaad G.F. and Abdel-Rahman R.F., Milk whey proteins modulate endotoxemia-induced hepatotoxicity in rats. *Int. J. Pharm. Pharm. Sci*., **7** (5), 65–71 (2015).
36. Zhang T., Liu H., Liu X-T.T., Xu D.R., Chen X.Q. and Wang Q., Qualitative and quantitative analysis of steroidal saponins in crude extracts from *Paris polyphylla* var. yunnanensis and *P. polyphylla* var. chinensis by high performance liquid chromatography coupled with mass spectrometry. *J. Pharm. Biomed. Anal*., **51** (1), 114–124 (2020).
37. Horai H., Arita M., Kanaya S., Nihei Y., Ikeda T., Suwa K., Ojima Y., Tanaka K., Tanaka S., Aoshima K., Oda Y., Kakazu Y., Kusano M., Tohge T., Matsuda F., Sawada Y., Hirai M.Y., Nakanishi H., Ikeda K., Akimoto N., Maoka T., Takahashi H., Ara T., Sakurai N., Suzuki H., Shibata D., Neumann S., Iida T., Tanaka K., Funatsu K., Matsuura F., Soga T., Taguchi R., Saito K., Nishioka T., MassBank: A public repository for sharing mass spectral data for life sciences. *J. Mass Spectrom*., **45** (7), 703–714 (2010).
38. MassBank of North America (MoNA), Fiehn Lab. https://mona.fiehnlab.ucdavis.edu/
39. Thu Z.M., Myo K.K., Aung H.T., Armijos C. and Vidari G., Flavonoids and stilbenoids of the genera Dracaena and Sansevieria: structures and bioactivities. *Molecules*, 25 (11), 2608-2634 (2020).
40. Allen F., Greiner R. and Wishart D., Competitive fragmentation modeling of ESI-MS/MS spectra for putative metabolite identification. *Metabolomics*, **11**, 98–110 (2015).
41. Allen F., Pon A., Wilson M., Greiner R. and Wishart D., CFM-ID: A web server for annotation, spectrum prediction and metabolite identification from tandem mass spectra. Nucleic Acids Res., 42: W94–W99 (2014).
42. Competitive Fragmentation Modeling-ID (CFM-ID), Wishartlab. https://cfmid.wishartlab.com/
43. El-Hawary S.S., El-Kammar H.A., Farag M.A., Saleh D.O. and El Dine R.S., Metabolomic profiling of five *Agave* leaf taxa via UHPLC/PDA/ESI-MS inrelation to their anti-inflammatory, immunomodulatory and ulceroprotective activities. *Steroids*, **160**, 108648 (2020).
44. De Combarieu E., Falzoni M., Fuzzati N., Gattesco F., Giori A., Lovati M. and Pace R., Identification of *Ruscus* steroidal saponins by HPLC-MS analysis. Fitoterapia, 73 (7-8), 583–596 (2002).
45. Mimaki Y., Takaashi Y., Kuroda M., Sashida Y. and Nikaido T., Steroidal saponins from *Nolina recurvata* stems and their inhibitory activity on cyclic AMP phosphodiesterase. *Phytochemistry*, **42** (6), 1609–1615 (1996).
46. Ahmad V.U., Basha A., editors. Ophiopogon Jaburan Saponin J-4. Spectrosc Data Steroid Glycosides Spirostanes, Bufanolides, Cardenolides. Boston, MA: Springer US, p. 1612–1613 (2006).
47. Mimaki Y., Kuroda M., Kameyama A., Yokosuka A. and Sashida Y., New steroidal constituents of the underground parts of *Ruscus aculeatus* and their cytostatic activity on HL-60 cells. *Chem. Pharm. Bull*., 46 (2), 298–303 (1998).
48. Le Tran Q., Tezuka Y., Banskota A.H., Tran Q.K., Saiki I. and Kadota S., New spirostanol steroids

and steroidal saponins from roots and rhizomes of *Dracaena angustifolia* and their antiproliferative activity. *J. Nat. Prod*., **64** (9), 1127–1132 (2001).
49. Kimura M., Tohma M., Yoshizawa I. and, Akiyama H., Constituents of *Convallaria*. X. Structures of Convallasaponin-A, -B, and Their Glucosides. Chem. Pharm. Bull. (Tokyo), 16 (1), 25–33 (1968).
50. Mimaki Y., Kuroda M.M., Fukasawa T. and Sashida Y., Steroidal Saponins from the bulbs of *Allium karataviense*. *Chem. Pharm. Bull. (Tokyo)*, 47 (6), 738–743 (1999).
51. Kanmoto T., Mimaki Y., Sashida Y., Nikaido T., Koike K. and Ohmoto T., Steroidal constituents from the underground parts of Reineckea carnea and their inhibitory activity on cAMP phosphodiesterase. *Chem. Pharm. Bull. (Tokyo)*, **42** (4), 926–931 (1994).
52. Liu H.W., Wang S.L., Cai B., Qu G.X., Yang X.J., Kobayashi H. and Yao, X-S., New furostanol glycosides from the rhizomes of *Dioscorea futschauensis* R. Kunth. *J. Asian Nat. Prod. Res*., 5 (4), 241-247 (2003).
53. Abu-Reidah I.M., Arráez-Román D., Segura-Carretero A. and Fernández-Gutiérrez A., Profiling of phenolic and other polar constituents from hydro-methanolic extract of watermelon (*Citrullus lanatus*) by means of accurate-mass spectrometry (HPLC-ESI-QTOF-MS). *Food Res. Int*., **51** (1), 354–62. (2013).
54. Harbaum B., Hubbermann E.M., Wolff C., Herges R., Zhu Z. and Schwarz K., Identification of flavonoids and hydroxycinnamic acids in pak choi varieties (*Brassica campestris* L. ssp. chinensis var. communis) by HPLC-ESI-MSn and NMR and their quantification by HPLC-DAD. *J. Agric. Food Chem*., **55** (20), 8251–8260 (2007).
55. Sánchez-Rabaneda F., Jáuregui O., Casals I., Andrés-Lacueva C., Izquierdo-Pulido M. and Lamuela-Raventós R.M., Liquid chromatographic/electrospray ionization tandem mass spectrometric study of the phenolic composition of cocoa (*Theobroma cacao*). *J. Mass Spectrom*., **38** (1), 35–42 (2003).
56. Hofmann T., Nebehaj E. and Albert L., Antioxidant properties and detailed polyphenol profiling of European hornbeam (*Carpinus betulus* L.) leaves by multiple antioxidant capacity assays and high-performance liquid chromatography/multistage electrospray mass spectrometry. Ind. Crops Prod., 87, 340–349 (2016).
57. Jaiswal R., Kiprotich J. and Kuhnert N., Determination of the hydroxycinnamate profile of 12 members of the Asteraceae family. Phytochemistry, 72 (8), 781–790 (2011).
58. Abu-Reidah I.M., Ali-Shtayeh M.S., Jamous R.M., Arráez-Román D. and Segura-Carretero A., HPLC-DAD-ESI-MS/MS screening of bioactive components from Rhus coriaria L. (Sumac) fruits. *Food Chem*., **166**, 179–191 (2015).
59. Ibrahim R.M., El-Halawany A.M., Saleh D.O., El Naggar E.M.B., EL-Shabrawy A.E.R.O. and El-Hawary S.S., HPLC-DAD-MS/MS profiling of phenolics from *Securigera securidaca* flowers and its anti-hyperglycemic and anti-hyperlipidemic activities. *Brazilian J. Pharmacogn*., **25** (2), 134–141 (2015).
60. Kang J., Price W.E., Ashton J., Tapsell L.C. and Johnson S., Identification and characterization of phenolic compounds in hydromethanolic extracts of sorghum wholegrains by LC-ESI-MSn. *Food Chem*., **211**, 215–226 (2016).
61. Schulze, A.E., HPLC method development for characterisation of the phenolic composition of *Cyclopia subternata* and *C. maculata* extracts and chromatographic fingerprint analysis for quality control, Thesis (MScFoodSc), Stellenbosch University(2013). Available from: https://core.ac.uk/download/pdf/37420288.pdf
62. Mokrani A., Cluzet S., Madani K., Pakina E., Gadzhikurbanov A., Mesnil M., Monvoisin A. and Richard T., HPLC-DAD-MS/MS profiling of phenolics from different varieties of peach leaves and evaluation of their antioxidant activity: A comparative study. *Int. J. Mass Spectrom*., **445**, 116192 (2019).
63. Kao T.H., Huang S.C., Inbaraj B.S. and Chen B.H., Determination of flavonoids and saponins in *Gynostemma pentaphyllum* (Thunb.) Makino by liquid chromatography-mass spectrometry. *Anal. Chim. Acta*., **626** (2), 200–211 (2008).
64. Spínola V., Pinto J. and Castilho P.C., Identification and quantification of phenolic compounds of selected fruits from Madeira Island by HPLC-DAD-ESI-MSn and screening for their antioxidant activity. Food Chem., 173, 14–30 (2015).
65. Brito A., Ramirez J.E., Areche C., Sepúlveda B. and Simirgiotis M.J., HPLC-UV-MS profiles of phenolic compounds and antioxidant activity of fruits from three *citrus* species consumed in Northern Chile. *Molecules*, **19** (11), 17400–17421 (2014).
66. Castelli M. V. and López S.N., Chapter 9 - Homoisoflavonoids: Occurrence, Biosynthesis, and Biological Activity. In: Atta-ur-Rahman BT-S in NPC, editor. Elsevier, p. 315–354 (2017).
67. Qi J., Xu D., Zhou Y-F., Qin M-J. and Yu B-Y., New features on the fragmentation patterns of homoisoflavonoids in *Ophiopogon japonicus* by high-performance liquid chromatography/diode-array detection/electrospray ionization with multi-stage tandem mass spectrometry. *Rapid*

Commun. Mass Spectrom., 24 (15), 2193–2206 (2010).
68. Ye M., Guo D., Ye G. and Huang C., Analysis of homoisoflavonoids in *Ophiopogon japonicus* by HPLC-DAD-ESI-MSn. *J. Am. Soc. Mass Spectrom*., **16** (2), 234–243 (2005).
69. Rivière C., Pawlus A.D. and Mérillon J-M., Natural stilbenoids: distribution in the plant kingdom and chemotaxonomic interest in Vitaceae. *Nat. Prod. Rep*., **29** (11), 1317–1334 (2012).
70. Sánchez-Rabaneda F., Jáuregui O., Lamuela-Raventós R.M., Viladomat F., Bastida J. and Codina C., Qualitative analysis of phenolic compounds in apple pomace using liquid chromatography coupled to mass spectrometry in tandem mode. *Rapid Commun. Mass Spectrom*., **18** (5), 553–563 (2004).
71. Fischer U.A., Carle R. and Kammerer D.R., Identification and quantification of phenolic compounds from pomegranate (*Punica granatum* L.) peel, mesocarp, aril and differently produced juices by HPLC-DAD-ESI/MSn. *Food Chem*., **127** (2), 807–821 (2011).
72. Maheshwari R., Shreedhara C., Polu P., Managuli R., Xavier S., Lobo R., Setty M. and Mutalik S., Characterization of the phenolic compound, gallic acid from *Sansevieria roxburghiana* schult and schult. f. rhizomes and antioxidant and cytotoxic activities evaluation. *Pharmacogn. Mag*., **13** (Suppl.3), S693–S699 (2017).
73. Kumar N. and Goel N., Phenolic acids: Natural versatile molecules with promising therapeutic applications. *Biotechnol. Reports*, **24**, e00370 (2019).
74. Turati F., Trichopoulos D., Polesel J., Bravi F., Rossi M., Talamini R., Franceschi S., Montella M., Trichopoulou A., La Vecchia C. and Lagiou P., Mediterranean diet and hepatocellular carcinoma. *J. Hepatol*., **60** (3), 606–611 (2014).
75. Saha P., Talukdar A.D., Nath R., Sarker S.D., Nahar L., Sahu J. and Choudhury M.D., Role of natural phenolics in hepatoprotection: a mechanistic review and analysis of regulatory network of associated genes. *Front. Pharmacol*., 10, 509–534 (2019).
76. Yang M., Wang X., Guan S., Xia J., Sun J., Guo H. and Guo D.A., Analysis of triterpenoids in *Ganoderma lucidum* using liquid chromatography coupled with electrospray ionization mass spectrometry. *J. Am. Soc. Mass Spectrom.*, **18** (5), 927–939 (2007).
77. Hou J., Dong H., Yan M., Zhu F., Zhang X., Wang H., Ye W. and Li P., New guaiane sesquiterpenes from *Artemisia rupestris* and their inhibitory effects on nitric oxide production. *Bioorg. Med. Chem. Lett*., **24** (18), 4435–4438 (2014).
78. Obul M., Wang X., Zhao J., Li G., Aisa H.A. and Huang G., Structural modification on rupestonic acid leads to highly potent inhibitors against influenza virus. *Mol. Divers*, **23**, 1–9 (2019).
79. Villasenor I., Bioactivities of Iridoids. *Antiinflamm. Antiallergy Agents Med. Chem*., **6** (4), 307–314 (2007).
80. Han H., Li Z., Gao Z., Yin X., Dong P., Yang B. and Kuang H., Synthesis and biological evaluation of picroside derivatives as hepatoprotective agents. Nat. Prod. Res., 33, 2845–2850 (2019).
81. Wu J-G., Kan Y-J., Wu Y-B., Yi J., Chen T-Q and Wu J-Z., Hepatoprotective effect of ganoderma triterpenoids against oxidative damage induced by tert -butyl hydroperoxide in human hepatic HepG2 cells. *Pharm. Biol*., **54** (5), 919–929 (2016).
82. Kim I.D. and Ha B.J., The effects of paeoniflorin on LPS-induced liver inflammatory reactions. *Arch Pharm. Res*., **33** (6), 959–966 (2010).
83. Francescato L.N., Debenedetti S.L., Schwanz T.G., Bassani V.L.and Henriques A.T., Identification of phenolic compounds in *Equisetum giganteum* by LC-ESI-MS/MS and a new approach to total flavonoid quantification. *Talanta*, 105, 192–203 (2013).
84. Marchetti L., Pellati F., Graziosi R., Brighenti V., Pinetti D. and Bertelli D., Identification and determination of bioactive phenylpropanoid glycosides of *Aloysia polystachya* (Griseb. et Moldenke) by HPLC-MS. *J. Pharm. Biomed. Anal*., 166, 364–370 (2019).
85. Ramadan A., Afifi N., Yassin N.Z., Abdel-Rahman R.F., Abd El-Rahman S.S. and Fayed H.M., Mesalazine, an osteopontin inhibitor: The potential prophylactic and remedial roles in induced liver fibrosis in rats. *Chem. Biol. Interact*., **289**, 109–118 (2018).
86. Ramadan A., Soliman G., Mahmoud S.S., Nofal S.M. and Abdel-Rahman R.F., Hepatoprotective and hepatotheraputic effects of propolis against d-galactosamine/lipopolysaccharide-induced liver damage in rats. *Int. J. Pharm .Pharm. Sci*., **7** (2), 372–378 (2015).
87. Ahmed S.M.U., Luo L., Namani A., Wang X.J. and Tang X., Nrf2 signaling pathway: Pivotal roles in inflammation. *Biochim. Biophys. Acta. Mol. Basis Dis*., **1863** (2), 585–597 (2017).
88. Bellezza I., Giambanco I., Minelli A. and Donato R., Nrf2-Keap1 signaling in oxidative and reductive stress. *Biochim. Biophys. Acta. Mol. Cell Res*., **1865** (5), 721–733 (2018).
89. Hennig P., Garstkiewicz M., Grossi S., Di Filippo M., French L. and Beer H-D., The Crosstalk

between Nrf2 and Inflammasomes. *Int. J. Mol. Sci*., **19** (2), 562-581 (2018).
90. Xu D., Xu M., Jeong S., Qian Y., Wu H., Xia Q. and Kong X., The role of Nrf2 in liver disease: novel molecular mechanisms and therapeutic approaches. *Front Pharmacol*., **9**, 1428-1235 (2019).
91. Hwang A-R., Han J-H., Lim J.H., Kang Y.J. and Woo C-H., Fluvastatin inhibits AGE-induced cell proliferation and migration via an ERK5-dependent Nrf2 pathway in vascular smooth muscle cells. *PLoS One*, **12** (5), e0178278 (2017).
92. Kundu J.K. and Surh Y-J., Nrf2-Keap1 signaling as a potential target for chemoprevention of inflammation-associated carcinogenesis. *Pharm. Res*., **27** (6), 999–1013 (2010).
93. Li L., Dong H., Song E., Xu X., Liu L. and Song Y., Nrf2/ARE pathway activation, HO-1 and NQO1 induction by polychlorinated biphenyl quinone is associated with reactive oxygen species and PI3K/AKT signaling. *Chem. Biol. Interact*, **209**, 56–67 (2014).
94. Sumi S.A., Siraj M.A., Hossain A., Mia M.S., Afrin S. and Rahman M.M., Investigation of the key pharmacological activities of *Ficus racemosa* and analysis of its major bioactive polyphenols by HPLC-DAD. *Evid. Based Complement Altern. Med.*, **2016**, 3874516 (2016).